



Volcanic Hazard Assessment at the Campi Flegrei Caldera, Italy

Andrea Bevilacqua, Giovanni Macedonio,
Augusto Neri, Giovanni Orsi,
and Paola Petrosino

Abstract

The Campi Flegrei caldera is a complex and resurgent structure, and its active portion has been the site of an intense volcanism with eruptions concentrated in temporal clusters, called epochs. The caldera is home to about 350,000 people. In the past decades, many scientific studies were aimed at both defining fundamental parameters of a future eruption, and hazard zoning of the territory. The approach to the volcanic hazard assessment of the Campi Flegrei caldera has progressively changed through time from a “deterministic” interpretation of the available information to a quantitative probabilistic elaboration of the main sources of uncertainty. In particular, on the long-term, Astroni-Agnano-Solfatara is recognised to be the most probable area in which a vent will likely open, while the Averno-Monte Nuovo is the second most

probable one. Significant uncertainty affects these results, and a non-negligible vent opening probability spreads over the whole caldera. The inter-event times of volcanic eruptions span from a few years to thousands of years. Within the epochs of activity, the mean recurrence time is tens of years, and intra-epoch temporal groups are evident. The probability that the next eruption will be of $< 0.1 \text{ km}^3$ volume of magma DRE is $\sim 95\%$. Larger size eruptions tend to be localised in the central-eastern sector of the caldera. Expected hazards from renewal of explosive volcanism result from pyroclastic fallout and pyroclastic density currents. Pyroclastic fallout deposits in excess of 300 kg/m^2 can affect most of the caldera and the city of Naples with more than 10% probability. The entire caldera has the potential to be affected by pyroclastic density currents invasion with mean probability above 30% in its central-eastern portion, and above 50% in the Agnano area. Invasion probabilities of $\sim 5\text{--}10\%$ have been estimated for the urbanised areas along the eastern slopes of the Posillipo Hill. In summary, probabilistic hazard assessment is particularly important in Campi Flegrei caldera, due to the uncertain location for potential vents and the large variability of eruption styles and sizes that cannot be, at the present time, effectively constrained by monitoring signals.

A. Bevilacqua (✉) · A. Neri
Istituto Nazionale di Geofisica e Vulcanologia,
Sezione di Pisa, Pisa, Italy
e-mail: andrea.bevilacqua@ingv.it

G. Macedonio
Istituto Nazionale di Geofisica e Vulcanologia,
Sezione Osservatorio Vesuviano, Napoli, Italy

G. Orsi · P. Petrosino
Dipartimento di Scienze della Terra, dell’Ambiente e
delle Risorse, Università degli Studi di Napoli
Federico II, Napoli, Italy

1 Introduction

At least 575 volcanoes, out of the over 1,250 that have been active in the Holocene, have erupted in historical times (Simkin and Siebert 1994; Brown et al. 2014; Siebert et al. 2015), and 97 out of 446 calderas are in unrest as of December 2020 (Newhall and Dzurisin 1988a, b; Geyer and Marti 2008; Siebert et al. 2010; Acocella et al. 2015; <https://volcano.si.edu/>). About 11% of the Earth population lives in a radius of 100 km around volcanoes that in the last 10,000 years have generated hazardous phenomena, able to adversely affect people, structures and infrastructures (Blong 1984; Small and Naumann 2001; Heiken et al. 2003; Marti and Ernst 2005; Aspinall and Blong 2015).

Modern volcanology tackled the challenge of eruption forecasting, assessing volcanic hazard, and zoning the exposed territory in relation to the likely effects produced by the expected volcanic phenomena (Sparks 2003; Aspinall et al. 2003; Connor et al. 2015; National Academy of Science 2017). A thorough volcanic hazard assessment has to answer three basic questions: when, where and how will next eruption occur. In a caldera or a volcanic field, the spatial assessment of future vent opening typically comes first. Therefore, three key forecasting issues naturally arise: (i) the spatial location of a new vent opening; (ii) the onset time, that is, the expected time before the beginning of the next eruption; (iii) the style and size of the expected hazardous phenomena, and the affected areas.

Volcanic hazard assessments are typically classified in two groups: long-term assessments and short-term assessments (Banks et al. 1989; Marzocchi and Bebbington 2012; Poland and Anderson 2020). Long-term hazard assessments are based on the assumption that the past is a key to understanding the future, implying that the expected phenomena will be similar to those generated by that specific volcano in the past and affect similar areas. To do so, it is fundamental to reconstruct the eruptive history of that volcanic system. Another assumption is the portion of the entire history of the volcano to be taken into account. In a caldera, this portion generally post-dates the last event that has generated a dramatic and significant change in the structural setting of

the entire volcanic system, including its magmatic feeding system, so as to determine a change in its behaviour. From a practical point of view, a long-term hazard assessment is a preparatory approach valid on a long-term perspective, which allows being ready in case of an impending eruption.

Instead, short-term hazard assessments are based on the investigation of phenomena acknowledged as precursors of past eruptions and on the definition of the current state of the volcano through monitoring data. They will complement existing hazard models during an eruptive crisis, given enough time to react. In closed conduit volcanoes, type, size and time-evolution of precursors of past eruptions are defined through geological and historical-documentary studies. The current state of a volcano is assessed by analysing the data collected by geophysical and geochemical monitoring networks and geological-structural surveys (McGuire et al. 1995; Scarpa and Tilling 1996; Sparks et al. 2012; Dempsey et al. 2020).

The knowledge of when, where, and how a future eruption will occur, along with socio-economic evaluations, is propaedeutic to the assessment of the risk related to the activity of a volcanic system (Fournier d'Albe 1979; Tilling 2001; ISDR 2005; Aspinall and Blong 2015). Volcanic hazard and risk assessment, as well as the zoning of the territory in relation to the expected hazards and related risks, are the essential requirements for a sound territorial planning and for actions aimed at volcanic risk mitigation by the civil authorities.

The Campi Flegrei caldera (CFc) is an active, complex and resurgent structure whose volcanic and deformation history is outlined in Chap. [Volcanic and Deformation History of the Campi Flegrei Volcanic Field, Italy](#). It is the site of widespread fumarole and thermal spring activity (see Chap. [The Hydrothermal System of the Campi Flegrei Caldera, Italy](#)) that has persisted for millennia, as testified by the name Campi Flegrei (Burning Fields in English), that was given to the area by the earliest Hellenic colonists in the eighth century BC (see Chap. [The Urban Development of Campi Flegrei, Italy](#)). The caldera floor is also affected by an ongoing resurgence through a series of

short-term events, also known as bradyseism, that have occurred at least since the 1950s (Del Gaudio et al. 2010; Ricco et al. 2019; Chaps. [The Permanent Monitoring System of the Campi Flegrei Caldera, Italy](#); [The Hydrothermal System of the Campi Flegrei Caldera, Italy](#); [Historic Unrest of the Campi Flegrei Caldera, Italy](#); [Source Modelling from Ground Deformation and Gravity Changes at the Campi Flegrei Caldera, Italy](#)), and that determine the current unrest state of the caldera. All these characteristics highlight that the magmatic system is active.

CFc is in unrest since decades, and its volcanism had a prevailing explosive character, therefore volcanic hazard potential is high. The active portion of the caldera, hosting a densely inhabited conurbation and the western neighbourhoods of the city of Naples, is home to about 350,000 people, meaning that volcanic risk is also very high. In such a situation, a volcanic hazard assessment and a zoning of the territory in relation to the expected hazardous phenomena in case of renewal of the activity in short- or mid-terms, is a must for the scientific community. In fact, in the past decades several scientific studies focussed on these topics have been published. The approach to the volcanic hazard assessment of the CFc has progressively changed through time from a “deterministic” interpretation of geological, volcanological, geochemical and geophysical data to a quantitative probabilistic elaboration of these data.

This Chapter presents the results achieved by the scientific community over the years and synthesises the current state of knowledge on the main topics needed for a comprehensive volcanic hazard assessment.

2 Volcanological Outlines

The CFc, the dominant feature of the CF volcanic field, was first interpreted by Orsi et al. (1992, 1996) as a nested, resurgent and restless structure resulting from two cataclysmic eruptions (see also Chap. [Volcanic and Deformation History of the Campi Flegrei Volcanic Field, Italy](#) and references therein; Fig. 1). The youngest caldera is

believed to be the only portion still active of the entire structure (Capuano et al. 2013).

The earliest caldera-forming event was the Campanian Ignimbrite (CI) eruption occurred around 40 ka (Barberi et al. 1978; Fisher et al. 1993; Orsi et al. 1996; Rosi et al. 1996; Civetta et al. 1997; Fedele et al. 2008; Perrotta et al. 2010; Giaccio et al. 2017; Silleni et al. 2020). The second event, with a collapse nested within the earlier one, was the Neapolitan Yellow Tuff (NYT) eruption that took place at about 15 ka (Orsi et al. 1992, 1995; Scarpati et al. 1993; Wohletz et al. 1995; Deino et al. 2004). A caldera collapse between these two has been recently hypothesised (Albert et al. 2019). Prior to the CI caldera collapse, the volcanism extended far outside the margins of the CFc, while after each collapse, it has been concentrated within the collapsed area. The stratigraphic sequence of the deposits of the pre-NYT activity and, thus, the volcanic history until the collapse of the NYT caldera is difficult to reconstruct in detail because of the large area affected by the CI caldera collapse, the huge amount of material deposited by the CI eruption, and the occurrence of the NYT caldera collapse over a large portion of the western sector of the CI caldera floor.

The NYT caldera collapse occurred through a piecemeal mechanism mostly along northeast-southwest and northwest-southeast, and subordinately north-south trending faults, likely reactivating portions of pre-existing regional structures (Capuano et al. 2013). The NYT eruption and related caldera collapse have produced such a remarkable change in the structural setting of the volcanic system to significantly modify its behaviour. The floor of the NYT caldera has been the site of an intense and interconnected deformation and volcanic activity. The main display of the deformation is an ongoing resurgence of the central portion of the caldera floor, while the volcanism has generated at least 70 eruptions in the last 15 kyrs.

Within the NYT caldera resurgence, a long-term and a short-term deformation have been distinguished; the long-term deformation sums up the effects of the short-term deformation, which occurs over years to tens of years, and accounts for

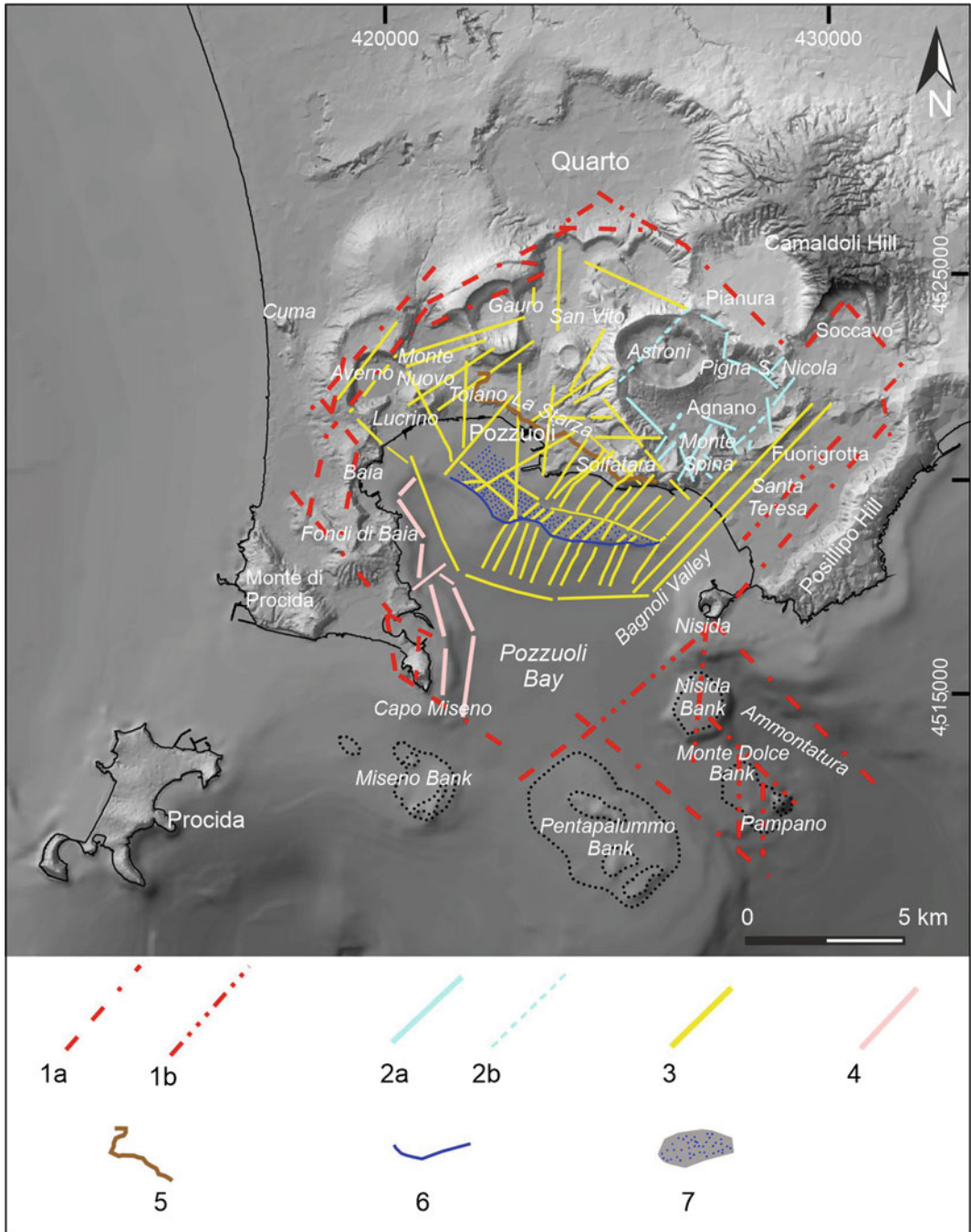


Fig. 1 Structural sketch map of the Neapolitan Yellow Tuff caldera. **1a** Faults active during the Neapolitan Yellow Tuff eruption. **1b** Faults likely active during the Neapolitan Yellow Tuff eruption. **2a** Faults active during the Agnano-Monte Spina eruption. **2b** Faults likely active during the Agnano-Monte Spina eruption. **3** Faults active during resurgence of La Starza block. **4** Faults active during subsidence of the Neapolitan Yellow Tuff caldera floor. **5** Rim of La Starza marine terrace. **6** Rim of the post-Würmian level surface. **7** Post-Würmian level surface. Figure modified after Chap. [Volcanic and Deformation History of the Campi Flegrei Volcanic Field, Italy](#)

the general process of resurgence operating since the NYT caldera collapse (Orsi et al. 1996, 1999). The long-term deformation has disjoined the caldera floor generating the uplifting of blocks in its central portion (Acocella 2010; Natale et al. 2020). The main expressions of this uplift are two parallel morphostructural features (Chap. [Volcanic and Deformation History of the Campi Flegrei Volcanic Field, Italy](#); Fig. 1). One is a northwest-southeast oriented on-land feature topped by the La Starza marine terrace for which a maximum net uplift of 85–100 m has been evaluated (Cinque et al. 1985; Sacchi et al. 2014; Isaia et al. 2019). A hypothetical maximum cumulative uplift of ~ 180 m has been estimated for the entire structure after the NYT caldera collapse (Sacchi et al. 2014). The second is the Lucrino-Bagnoli Valley morphostructural high, delimited towards the southwest by a roughly northwest-southeast trending alignment of high-angle morphostructural slopes and truncated by a post-Würmian level surface in the Pozzuoli Bay (Chap. [Volcanic and Deformation History of the Campi Flegrei Volcanic Field, Italy](#); Fig. 1).

The short-term deformation (i.e., the bradyseism) is interpreted as transient episodes during the general resurgence process (Orsi et al. 1999; Del Gaudio et al. 2010). These events generate ground deformation, seismicity, gravity changes and compositional variations of fluid effluents (for reviews see Chaps. [The Permanent Monitoring System of the Campi Flegrei Caldera, Italy](#); [The Hydrothermal System of the Campi Flegrei Caldera, Italy](#); [Historic Unrest of the Campi Flegrei Caldera, Italy](#); [Source Modelling from Ground Deformation and Gravity Changes at the Campi Flegrei Caldera, Italy](#), and references therein). In 2012 values and trends of these phenomena induced the Italian Dipartimento della Protezione Civile to raise the alert level from “base” to “attention” (www.protezionecivile.it).

2.1 Post-Neapolitan Yellow Tuff Volcanism

The post-NYT volcanism was fed by a complex feeding system, and extruded magmas varying in

composition from trachybasalt to phonolite (Chaps. [An Evolutionary Model for the Magmatic System of the Campi Flegrei Volcanic Field \(Italy\) Constrained by Petrochemical Data](#); [Origin and Differentiation History of the Magmatic System Feeding the Campi Flegrei Volcanic Field \(Italy\) Constrained by Radiogenic and Stable Isotope Data](#); [Tephrochronology and Geochemistry of Tephra from the Campi Flegrei Volcanic Field, Italy](#)). Their time sequence, reported in Table 1, is derived from the current literature (e.g., Orsi et al. 2004; Smith et al. 2011; Fedele et al. 2011, 2012; Isaia et al. 2012; Bevilacqua et al. 2015, 2016). The eruptions over the past 15 kyrs occurred in three clusters of activity, called epochs, followed by periods of quiescence (Di Vito et al. 1999). After more than 3 kyrs of quiescence following the end of the last epoch, the Monte Nuovo last eruption occurred as a solitary event in AD 1538 (Guidoboni and Ciuccarelli 2011; Di Vito et al. 2016 and references therein).

During each epoch of activity, the eruptions followed each other with time intervals of tens to hundreds of years. The distribution of the active vents through time has followed a specific pattern in each epoch of activity (Figs. 2 and 3) and has been considered as a tracer of the structures acting as feeding features for volcanism (Orsi et al. 1996, 1999, 2004).

The eruptions of the past 15 kyrs of the CFC were predominantly explosive, with only four effusive events (Table 1). The effusive eruptions mostly extruded dense trachytic magmas that formed lava domes and subordinately short and stubby lava flows. The explosive eruptions were characterised by phreatomagmatic phases prevailing over purely magmatic. Contemporaneous magmatic and phreatomagmatic explosions have also been documented (Dellino et al. 2004; Romano et al. 2020). The phreatomagmatic explosions generated mostly dilute pyroclastic density currents (PDCs) that flowed within the floor of the NYT caldera and in some cases overcame its high-angle morphological boundaries to spread over the surrounding plain (Fig. 4). The magmatic explosions gave rise to

Table 1 Post-NYT eruptions

ID	Eruption	Epoch	Age (cal. years BP)		Magma Volume (DRE) (km ³)			Area PDC (km ²)
			Percentile		Percentile			
			2.5th	97.7th	5th	50th	95th	
70	Monte Nuovo	AD 1538			0.03	0.03	0.03	5.7
69	Nisida	3b	3,213	4,188	0.01	0.02	0.03	4.7
68	Fossa Lupara	3b	3,978	4,192	0.01	0.02	0.03	8.9
67	Astroni 7	3b	4,098	4,297	0.04	0.07	0.11	10.2
66	Astroni 6	3b			0.06	0.12	0.18	26.9
65	Astroni 5	3b			0.05	0.10	0.15	29.1
64	Astroni 4	3b			0.07	0.14	0.21	60.4
63	Astroni 3	3b			0.08	0.16	0.24	41.1
62	Astroni 2	3b			0.01	0.02	0.03	19.1
61	Astroni 1	3b	4,153	4,345	0.03	0.06	0.09	39.7
60 [?]	Capo Miseno	3b	3,200	4,200	0.01	0.02	0.03	1.1
59 ^a	Averno 2	3b			0.04	0.07	0.11	24.8
58	Solfatara	3b	4,181	4,386	0.02	0.03	0.05	8.7
57 ^b	Accademia Lava Dome	3b			0.00	-	0.01	
56	Monte Olibano Tephra	3b			0.01	-	0.10	
55	Solfatara lava dome	3b			0.00	-	0.01	
54	Paleo-Astroni 3	3b			0.01	0.02	0.03	
53 ^b	M.te Olibano Lava Dome	3b			0.00	-	0.01	
52	S.ta Maria delle Grazie	3b	4,382	4,509	0.01	-	0.10	
51	Agnano-Monte Spina	3a	4,482	4,625	0.43	0.85	1.28	312.5
50	Paleo-Astroni 2	3a	4,712	4,757	0.10	-	0.30	5.4
49	Paleo-Astroni 1	3a	4,745	4,834	0.03	0.05	0.08	18.1
48 ^b	Monte Sant'Angelo	3a	4,832	5,010	0.10	-	0.30	43.8
47	Pignatiello 2	3a			0.01	0.02	0.03	
46	Cigliano	3a			0.03	0.05	0.08	28.3
45	Agnano 3	3a			0.10	0.19	0.29	68.0
44	Averno 1	3a	5,064	5,431	0.01	-	0.10	27.0
43	Agnano 2	3a			0.01	0.01	0.02	17.1
42	Agnano 1	3a	5,266	5,628	0.01	0.02	0.03	
41	San Martino	2	9,026	9,370	0.03	0.05	0.08	19.7
40	Sartania 2	2			0.01	-	0.10	27.0
39	Pigna San Nicola	2	9,201	9,533	0.10	-	0.30	8.0
38	Costa San Domenico	2			0.01	-	0.10	16.9
37	Monte Spina Lava Dome	2			0.00	-	0.01	
36	Sartania 1	2	9,500	9,654	0.01	-	0.10	40.7
35	Fondi di Baia	2	9,525	9,695	0.02	0.04	0.06	15.7
34	Baia	2			0.00	-	0.01	
33 [?]	Porto Miseno	1	10,347	12,860	0.01	-	0.10	0.7
32 [?]	Bacoli	1	11,511	14,154	0.10	0.20	0.30	1.1

(continued)

Table 1 (continued)

ID	Eruption	Epoch	Age (cal. years BP)		Magma Volume (DRE) (km ³)			Area PDC (km ²)
			Percentile		Percentile			
			2.5th	97.7th	5th	50th	95th	
31	Casale	1			0.01	-	0.10	
30	Pisani 3	1	10,516	10,755	0.01	-	0.10	3.0
29	Pignatiello 1	1			0.01	-	0.10	
28	Montagna Spaccata	1			0.01	0.02	0.03	3.0
27	Concola	1			0.00	-	0.01	
26	Fondo Riccio	1			0.00	-	0.01	
25	Pisani 2	1			0.10	-	0.30	21.1
24	Pisani 1	1			0.10	-	0.30	
23	Soccavo 5	1			0.01	-	0.10	66.2
22	Minopoli 2	1			0.01	-	0.10	113.6
21	Paleo-San Martino	1			0.01	-	0.10	37.3
20	Soccavo 4	1			0.10	-	0.30	180.2
19	S4s3_2	1			0.01	-	0.10	
18	S4s3_1	1			0.10	-	0.30	
17	Soccavo 3	1			0.01	-	0.10	147.5
16	Soccavo 2	1			0.01	-	0.10	75.8
15	Paleo-Pisani 2	1			0.10	-	0.30	37.7
14	Paleo-Pisani 1	1			0.01	-	0.10	190.5
13	Pomici Principali	1	11,915	12,158	0.43	0.85	1.28	129.2
12	Gaiola	1			0.01	-	0.10	
11	Soccavo 1	1			0.25	0.50	0.75	190.5
10	Paradiso	1			0.01	-	0.10	
9	Minopoli 1	1			0.01	-	0.10	
8	Torre Cappella	1			0.01	-	0.10	1.0
7	La Pigna 2	1			0.01	-	0.10	
6	La Pigna 1	1	12,749	13,110	0.01	-	0.10	
5	La Pietra	1			0.01	-	0.10	2.6
4	Santa Teresa	1			0.01	-	0.10	0.9
3	Gauro	1	12,721	15,511	0.25	0.50	0.75	16.1
2	Mofete	1			0.01	-	0.10	2.1
1	Bellavista	1			0.01	-	0.10	3.9

Legend: ^acoeval with the previous eruption; ^buncertain stratigraphic order with the previous eruption; [?]unconstrained stratigraphic order. The eruptions record is based on Di Vito et al. (1999), de Vita et al. (1999), Isaia et al. (2004, 2009), Orsi et al. (2004, 2009), Di Renzo et al. (2011), Fedele et al. (2011), Smith et al. (2011), Neri et al. (2015a, b) and Bevilacqua et al. (2016). The Age and Magma Volume estimates are from Smith et al. (2011) and references therein. The Age of Capo Miseno is from Di Renzo et al. (2011). The Magma Volume uncertainty ranges are from Bevilacqua et al. (2016). The Area PDC estimates are from Orsi et al. (2004) but those of events 33, 15, 8, 4 that are from Neri et al. (2015a, b), and the one of event 51 that is from de Vita et al. (1999)

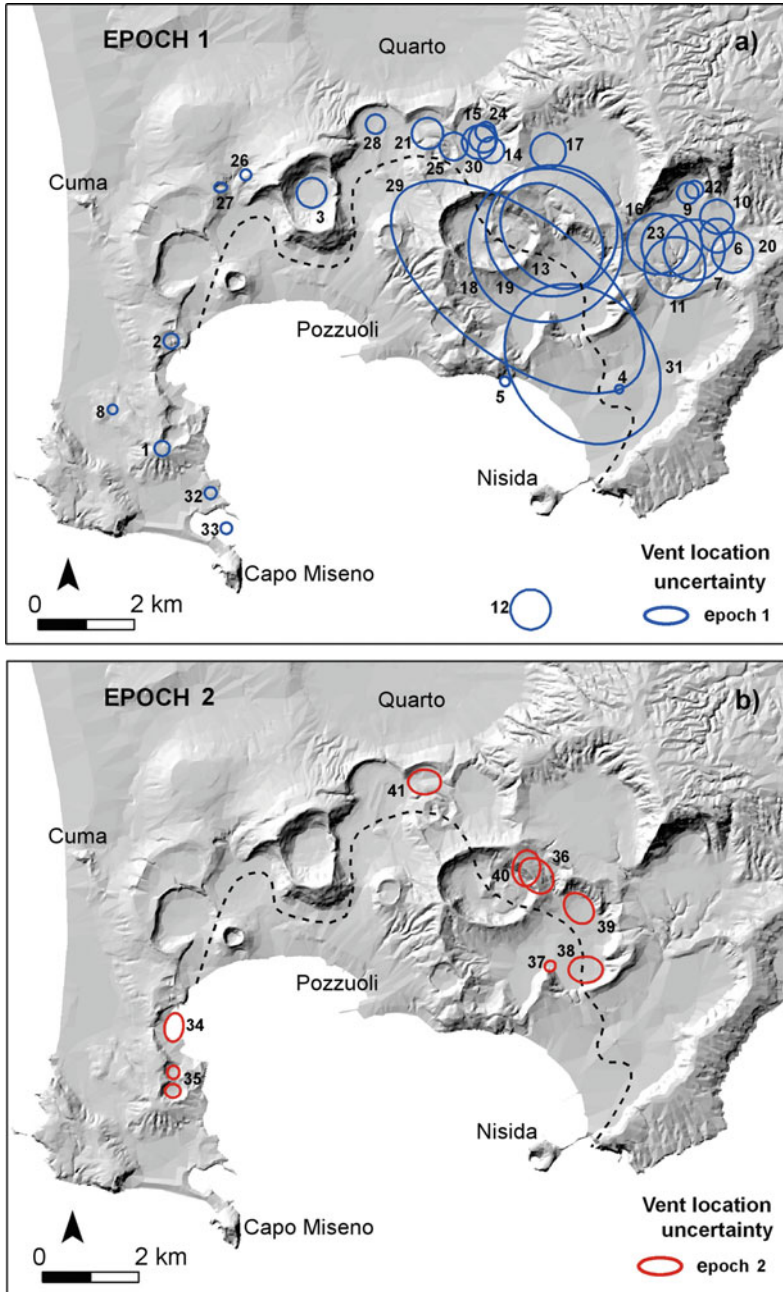
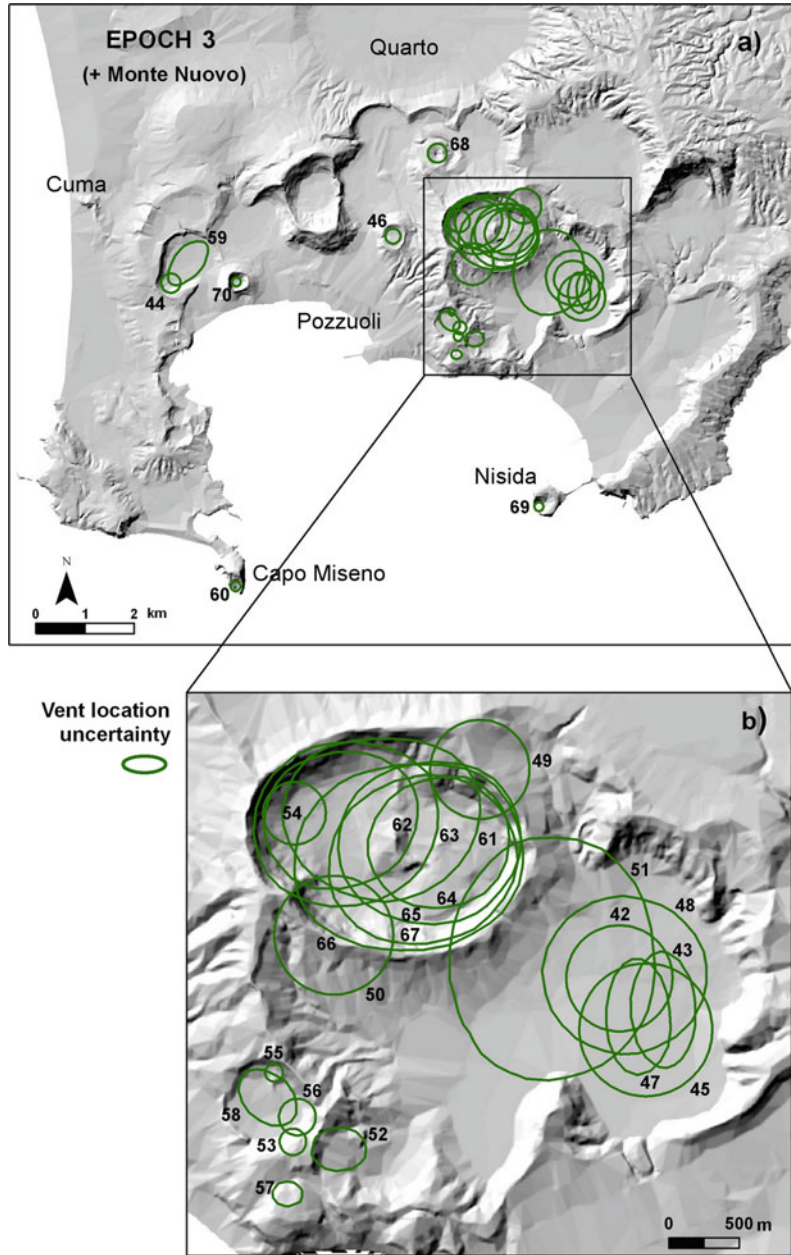


Fig. 2 Location of the vents of the eruptions of **a** epoch 1 and **b** epoch 2. Numbering of the events follows Table 1. The dashed line indicates the likely location of the coast line between epochs 2 and 3 (modified after Orsi et al. 2004). Figure modified after Bevilacqua et al. (2015)

Fig. 3 **a** Location of the vents of the eruptions of epoch 3. **b** zoom of **a**. Numbering of the events follows Table 1. Figure modified after Bevilacqua et al. (2015)



sustained columns that laid down pyroclastic fallout (PF) beds mostly easterly dispersed (Fig. 5). In a few cases, they also generated dense PDCs.

Most of the explosive eruptions varied from low- to medium-magnitude events (Table 1); only three in epoch 1 and one in epoch 3 had a magnitude significantly higher. There is no clear relationship between the length of a period of

quiescence and the size of the first eruption of the following epoch. Furthermore, the first eruption has never been the highest magnitude event of any of the three epochs (Orsi et al. 2003, 2004). An estimate of the temporal rate of the erupted volume in the epochs of activity was obtained, with uncertainty quantification (Fig. 6; Bevilacqua et al. 2016). An intensification of the activity rate with time was remarked during epochs 1 and 3, an

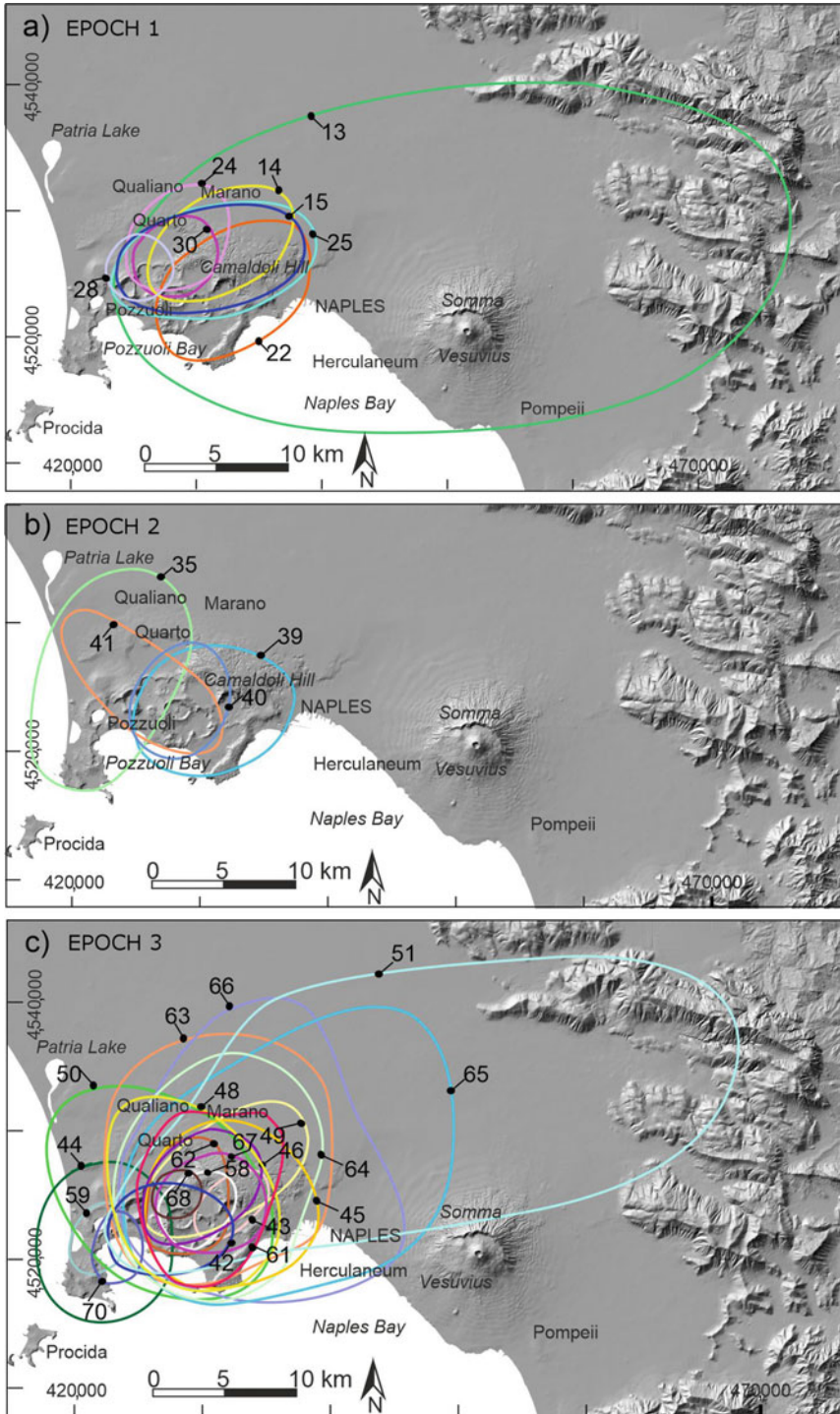


Fig. 4 10-cm isopachs of the pyroclastic fallout deposits of **a** epoch 1, **b** epoch 2, and **c** epoch 3 and Monte Nuovo. **d** zoom of the Campi Flegrei area in **c**. Numbering of the events follows Table 1. Figure modified after Orsi et al. (2004)

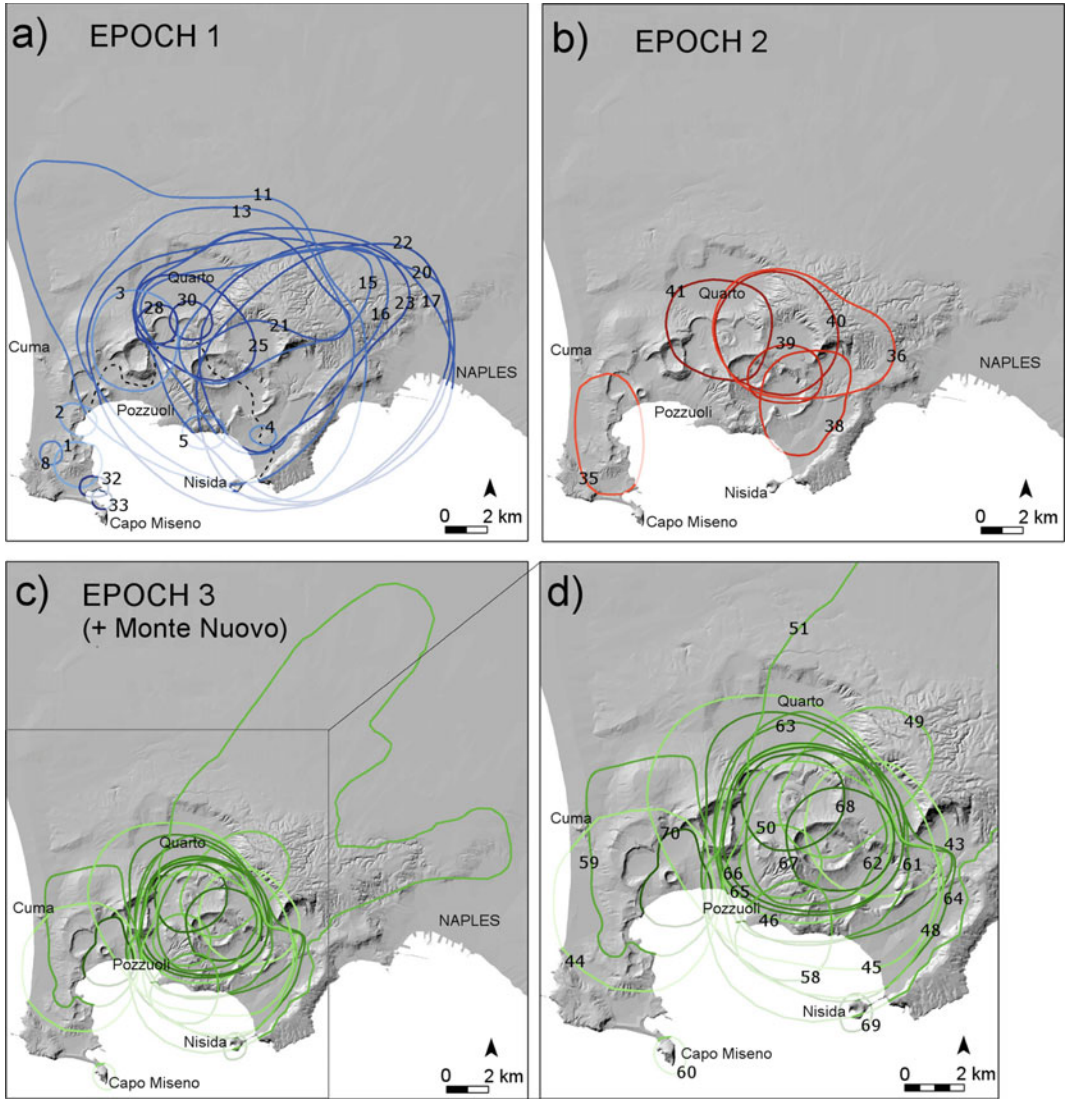


Fig. 5 Distribution of pyroclastic density current deposits of the eruptions of **a** epoch 1, **b** epoch 2, and **c** epoch 3 plus the Monte Nuovo event. Numbering of the events follows Table 1. Different colour tones indicate

apparent feature despite the large uncertainties affecting the age of the oldest events of epoch 1. It was not possible to clearly identify similar features in the much shorter epoch 2, due to the uncertainty affecting time and size of the eruptions.

Some eruptions have shown peculiar characteristics, such as contemporaneous events in distinct portions of the caldera floor, migration of the vent during a single event, building of a volcano through several eruptions close in time

different events. Reported deposit boundaries were extended overseas to allow estimation of reasonable values for pyroclastic density current invasion area. Figure modified after Neri et al. (2015a, b)

and space, and occurrence of a structural collapse during the event.

2.1.1 Epoch 1

Epoch 1, lasted from the NYT eruption to ~10.6 ka, generated at least 33 eruptions largely varied in size that followed each other at mean time intervals of about 80–140 years, and erupted a volume of magma of $4.2 \pm 0.7 \text{ km}^3$ DRE (Table 1; Fig. 2c; Bevilacqua et al. 2016; see

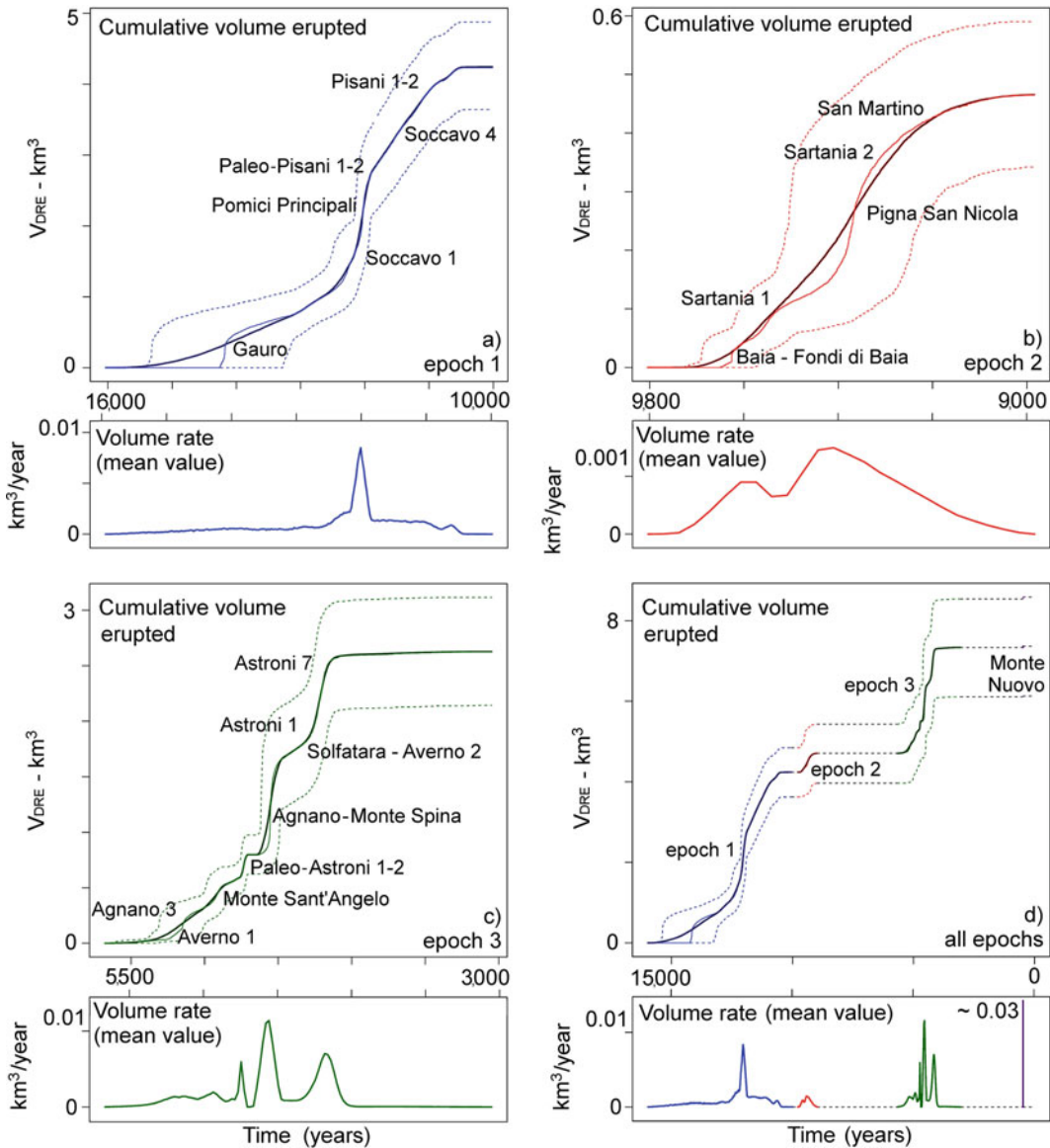


Fig. 6 Cumulative volume erupted as a function of time during **a** epoch 1 in blue, **b** epoch 2 in red, and **c** epoch 3 in green, and **d** the entire post-NYT activity (including Monte Nuovo in dark violet), assuming the described probability model. The bold line is the mean value, the narrow line is the 50th percentile and the dashed lines are the 5th and 95th percentiles of the epistemic uncertainty.

The event labels correspond to the largest eruptions of each epoch. Under the main plots are reported the time derivatives of the mean graphs, which represent the mean erupted volumes rate per year. It should be noted that such mean eruption volume rates are directly affected by the uncertainty associated to each event age. Figure modified after Bevilacqua et al. (2016)

Chap. **Volcanic and Deformation History of the Campi Flegrei Volcanic Field, Italy** and references therein). During this epoch, the vents were located along the structural boundary of the NYT caldera, with an apparent concentration in the

northern and north-eastern sectors. The earliest known activity of this epoch built up the Bellavista tuff cone through phreatomagmatic explosions that generated a zeolitised sequence of fine- to coarse-ash, mostly plain-parallel to

cross-laminated beds (Di Vito et al. 1999). The largest eruptions were Pomici Principali, Gauro, and Soccavo 1. The maximum rate of activity appeared to be reached with the Pomici Principali event and maintained for most of the second part of this epoch. The Pomici Principali event laid down a sequence, from base upward, of fine-ash fallout beds, pumice lapilli layers with subordinate ash beds that in proximal area show sedimentological characteristics of surge deposits, and fine-ash surge beds rich in accretionary lapilli. The three eruptions of Montagna Spaccata, Fondo Riccio, Concola in epoch 1 are suspected to have been contemporaneous (Rosi and Sbrana 1987). A few post-NYT events occurred in the submerged portion of the caldera (e.g., Nisida Bank) and their stratigraphic correlations are the subject of recent research (e.g., Steinmann et al. 2018; Chap. [Volcanic and Deformation History of the Campi Flegrei Volcanic Field, Italy](#)). This epoch likely ended with the growth of the Porto Miseno tuff ring, composed of a sequence of zeolitised plain parallel to cross-laminated, fine- to coarse-ash beds (Fedele et al. 2011). During the quiescence between epochs 1 and 2, which lasted between 0.8 and 1.1 ka, Paleosol A formed. It is largely exposed in the Neapolitan-Phlegraean area with variable thickness, and ranges in colour from light- to dark-brown.

2.1.2 Epoch 2

Epoch 2, lasted from ~ 9.6 to ~ 9.2 ka, was characterised by a minimum of 8 eruptions which occurred at mean time intervals of 35–75 years (Table 1; Fig. 2b; see Chap. [Volcanic and Deformation History of the Campi Flegrei Volcanic Field, Italy](#) and references therein). All eruptions but one were explosive, low magnitude events characterised by phreatomagmatic dominating over magmatic phases. They extruded a volume of magma of 0.5 ± 0.1 km³ DRE (Bevilacqua et al. 2016). The only effusive eruption generated the Monte Spina lava dome. The few vents active during epoch 2 were mostly located along the north-eastern and the western portions of the structural boundary of the NYT caldera. The epoch began with the Fondi di Baia

eruption that formed an eight-shaped tuff cone (Di Vito et al. 1999; Pistolesi et al. 2017; Voloschina et al. 2018). This eruption produced mostly phreatomagmatic and subordinately magmatic explosions that generated a sequence of sandwave, ash surge beds with coarse fallout layers in its basal portion. The highest magnitude event of this epoch was the Pigna San Nicola eruption (Di Vito et al. 1999). It was characterised by alternating magmatic and phreatomagmatic explosions, and formed a tuff cone, only partly preserved today. The deposits are a sequence of pumice lapilli and subordinate ash fallout beds topped by sandwave, fine- to coarse-ash surge deposits. The last event was the San Martino eruption (Di Vito et al. 1999), which alternated magmatic and phreatomagmatic explosions. This activity produced a sequence of fallout layers alternating to thin, mostly ash surge beds, with the pumice fallout dominating over the PDC deposits within the mid-lower portion of the sequence. A quiescence lasting between 3.5 and 4.0 kyrs followed this epoch of activity during which the widely exposed yellowish-brown Paleosol B formed.

2.1.3 Epoch 3

Epoch 3, lasted from ~ 5.5 to ~ 3.5 ka, produced at least 28 eruptions at mean time intervals of 50–80 years (Table 1; Fig. 2a; see Chap. [Volcanic and Deformation History of the Campi Flegrei Volcanic Field, Italy](#) and references therein). These eruptions were fed by 2.6 ± 0.5 km³ of magma DRE (Bevilacqua et al. 2016). A further twofold subdivision of this epoch in relation to a second-order pause in the activity, at ~ 4.4 ka, has also been suggested (Isaia et al. 2009). Most of epoch 3 vents were concentrated in the central-eastern portion of the NYT caldera floor, but the vents of the two Averno and the Monte Nuovo eruptions were in the north-western sector of the caldera, while those of the Nisida and Capo Miseno eruptions were at the south-western and south-eastern edges of the emerged portion of the caldera. The large majority of the eruptions of this epoch were explosive, with only 3 effusive events: namely Monte Olibano, Solfatara, and Accademia lava

domes, from the oldest to the youngest. The epoch began with the Agnano 1 eruption characterised by phreatomagmatic and magmatic explosions (Di Vito et al. 1999). These explosions produced a sequence of ash and pumice-lapilli fallout beds containing abundant ash particles, which becomes a thin ash layer in distal areas. The highest-magnitude event was the Agnano-Monte Spina (A-MS) eruption, accompanied by a volcano-tectonic collapse in the north-eastern portion of the NYT caldera (de Vita et al. 1999). The change in the eruption rate appears to coincide with this eruption, which somehow marks the subdivision of the epoch in two sub-epochs (Isaia et al. 2009). A-MS was characterised by phreatomagmatic and magmatic, sometimes contemporaneous, explosions that produced PDCs at variable particle concentrations and two sustained columns. The latter were generated during the eruption phases named B1 and D1, and reached height of 23 and 27 km, respectively (de Vita et al. 1999). The high particle concentration PDCs were confined within the caldera depression, while the more diluted ones overtopped the caldera boundaries and flowed for about 15 km within the surrounding plain. The sustained columns laid down easterly-to-northeasterly dispersed pumice fall deposits not less than 10 cm thick at about 42 km from the vent. The sequence is cut by an erosional unconformity, suggesting a time break in the eruption. A volcano-tectonic collapse likely occurred during this pause in the eruption. It affected an area of about 6 km², polygonal in shape, roughly northwest-southeast oriented, and located towards the north-eastern border of the NYT caldera floor.

The eruptions of Averno 2 and Solfatara, postdating the A-MS eruption and volcano-tectonic collapse, likely occurred contemporaneously (Isaia et al. 2009; Pistolesi et al. 2016). Their vents were located about 5 km apart, at the opposite sides of the north-south Pozzuoli structure that affects the NYT caldera floor (Capuano et al. 2013). The Averno 2 eruption (Di Vito et al. 2011) was characterised by a sequence of magmatic and phreatomagmatic explosions generating sustained and collapsing columns that

laid down PF and PDC deposits, prevailing during the first and the second part of the eruption, respectively. The maximum height reached by the sustained columns was about 10 km, and the vent migrated over a limited area during the eruption. The Solfatara eruption was characterised by phreatomagmatic with subordinate magmatic explosions that generated a sequence of surge beds with minor PF deposits (Rosi and Sbrana 1987; Isaia et al. 2015; Pistolesi et al. 2016). The Astroni volcano (Di Vito et al. 1999; Isaia et al. 2004; Tonarini et al. 2009) grew through 7 distinct eruptions occurred in a time span not longer than 300 years. The eruptions were dominantly phreatomagmatic, with generation of ashy PDCs; a sustained column formed only during eruption 6 and laid down a sub-Plinian pumice fall deposit. The eruption vent of each of the seven events, although confined within the 3 km² area of the present crater, migrated during the activity roughly from southeast to northwest. The vent of the Averno 2 eruption also migrated along a 2-km-long northeast-southwest oriented system of fractures.

3 Long-Term Assessment of Volcanic Hazard

Pioneering hazard assessment studies at the CFc were based on the “deterministic” reconstruction of reference events from the past. In particular, during the 1982–1984 bradyseismic crisis, Rosi and Santacroce (1984) considered three reference scenarios: a phreatic explosion like the AD 1198 event at the Solfatara volcano (Scandone et al. 2010), a low-magnitude explosive eruption like the AD 1538 Monte Nuovo event (Guidoboni and Ciuccarelli 2011; Di Vito et al. 2016 and references therein), and a maximum expected eruption like the A-MS event (de Vita et al. 1999). The spatial definitions of the hazardous phenomena were based on the areal distribution of the deposits of the reference events. Orsi et al. (2004) performed the first comprehensive eruption forecasting and hazard assessment at the restless CFc using stratigraphic, volcanological, structural and petrological data. Due to the

remarkable change in the structural setting of the CFc system produced by the NYT eruption and related caldera collapse, the authors assumed the entire history of the CFc system subsequent to these events as reference for volcanic hazard assessment. More recently, the approach to the volcanic hazard assessment has changed to include probabilistic forecasts that incorporate a variety of numerical modelling of past hazardous phenomena, along with the uncertainty quantification.

The expected phenomena in case of renewal of the volcanic activity of the CFc have various intensities and impacts depending on the style and size of the next eruption. This section describes the researches developed in the last two decades aimed at both defining fundamental parameters of a future eruption of the CFc and zoning of the territory in relation to the expected volcanic hazards. These results include vent location, time, size, and style of a future eruption.

3.1 Site of a Future Eruption and Vent Opening Probability Maps

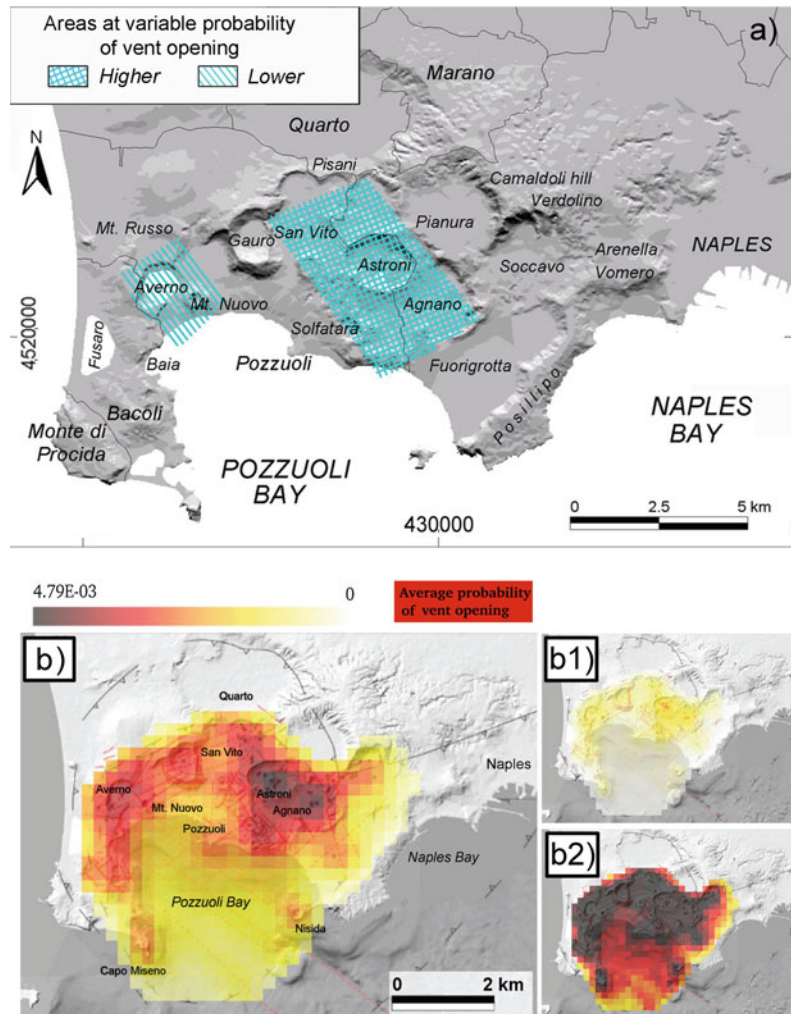
Alberico et al. (2002) were the first to quantify potential new vent openings at CFc. They subdivided the subaerial CF area into a regular grid of 1 km cells and evaluated the relative spatial probability of vent opening based on geological, geophysical and geochemical data. In particular, they included earthquake epicentres, gravity anomalies, along with location of past vents, recent faults, helium concentration anomalies, and fumaroles. The number of these elements present in a cell empirically defined a score for each cell of the grid. After a normalisation step, this score provided the probability of vent opening in each cell. The probability distribution spread over the whole NYT caldera, and had maximum values (above 1.6% over km²) in the central part, near Solfatara and Monte Nuovo.

Orsi et al. (2004) applied a different approach taking into consideration both history and current dynamics of the system. They inferred that if the

next eruption is triggered by the ongoing dynamics of the NYT caldera, the most likely new vent location would be in the north-eastern sector of the caldera. They correlated this area to the portion of the resurgent block under extension that has been the site of the majority of the eruptions of the past 5 kyrs (Fig. 2a). However, they did not exclude that a future vent could open in the Monte Nuovo-Averno Lake area, at the intersection of faults within the resurgent block with those bordering the block towards the northwest. They finally delimited one area of “higher” and one of “lower” probability of vent opening (Fig. 7a).

A new spatial probability map of vent opening was developed by Selva et al. (2012a) following a Bayesian approach based on Dirichlet random variables corresponding to 700 cells with 500-m sides in a rectangular grid covering the NYT caldera. A prior distribution was defined using an empirical procedure based on the association of unequal scores to the geological features present in a given spatial cell. These features included, with score points in parentheses: past vents (3 points), faults (2 points), and location within the NYT caldera (1 point). This procedure was simplified with respect to that of Alberico et al. (2002), in order to avoid the influence of modern unrest signals on a long-term, vent-opening probability map. The prior model was then combined with the likelihood of the number of epoch 3 vents in each cell. Vent migration during an eruption was not considered as indicative of multiple events, but the seven eruptions building up the Astroni volcano were considered as distinct events. This likelihood was defined according to a multinomial distribution, and the resulting probability was smoothed by using a Gaussian filter with a 2σ radius of 1 km, in order to reduce scatter and to cope with the spatial uncertainty affecting the data and the prior distribution. These maps (Fig. 7b) showed a sickle-shaped region of increased probability of vent opening, following the inland portion of the caldera, from Agnano to Baia, and including the Solfatara crater. Maximum values of $\sim 2\%$ probability over km² were calculated in the area of the Astroni volcano and the Agnano volcano-

Fig. 7 **a** Areas at variable probability of vent opening in case of renewal of volcanism in short-mid-terms at the Campi Flegrei caldera (modified after Orsi et al. 2004). **b**, **b1**, **b2** Conditional probability of vent opening at the Campi Flegrei caldera of the posterior filtered model. The average (best guess) value is shown in **b**, while **b1** and **b2** show the 10th and 90th percentiles confidence interval, respectively (modified after Selva et al. 2012a)

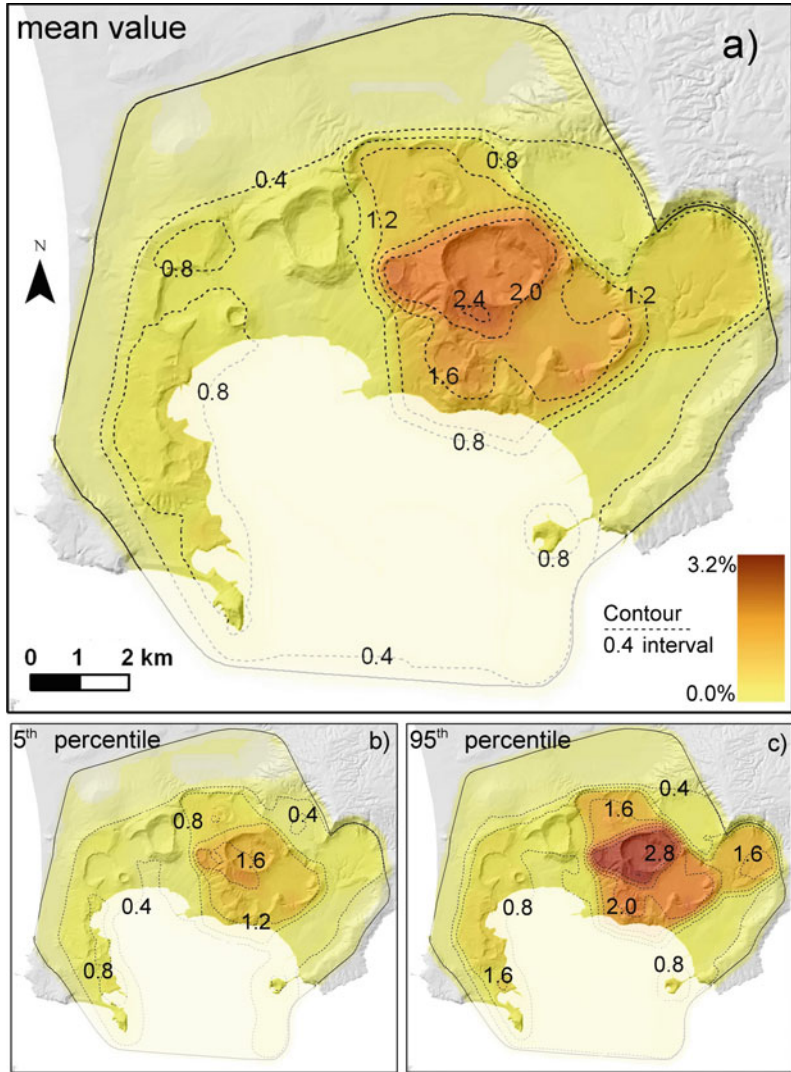


tectonic depression. The authors provided additional maps of the 10th and 90th percentiles of the uncertain probability values over the cells (Fig. 7b1, b2). Uncertainty ranged from +180% to -90% of the local mean values.

Bevilacqua et al. (2015) developed a more comprehensive vent opening probability map for a future eruption within the CFc, through a weighted linear combination of five maps describing the spatial distribution of relevant volcanic features. Such features included the eruption vent locations of the past 15 kyrs (each epoch was separately considered; Fig. 2), and the maximum fault displacement and the surface fractures density from Vitale and Isaia (2014). A uniform probability map within the caldera

was included to account for unconsidered or unidentified processes and variables. The past vent locations were represented by ellipses defining the associated uncertainty area, rather than by deterministic points. Their density distribution was processed using either Gaussian kernel functions or a partitioning of the caldera into sixteen homogeneous zones, with quite consistent results. An uncertain number of “lost vents” with unconstrained location in the sub-aerial part of the caldera was also included in the analysis. The uncertain weights to be associated with the features that contributed to the definition of the vent opening map relied on expert judgment techniques (see also Aspinall and Cooke 2013; Bevilacqua 2016). Based on the expert

Fig. 8 Probability maps of new vent opening as obtained weighting the six variable distributions considered in Bevilacqua et al. (2015). Contours and colours indicate the percentage probability of vent opening per km² (conditional on the occurrence of an eruption). **a** Mean values, **b** and **c** 5th and 95th percentile values, respectively. Figure modified after Bevilacqua et al. (2015)



elicitation outcomes, areal distribution of previous vents was judged the most important variable for quantifying the vent opening probability map, with a total contribution weight of about 47% (mean value). The distributions of the maximum fault displacement and surface fracture density were weighted about 16% and 12%, respectively. About 25% weight was assigned to the uniformly homogeneous spatial vent opening map (i.e., to the possibility that the next vent could open anywhere inside the NYT caldera). The results, expressed as a mean probability map and 5th and 95th uncertainty percentiles of the probability values, outlined a main, quite wide, region in the

central-eastern part of the caldera characterised by the highest probabilities of vent opening (Fig. 8). The maximum probabilities were between 1.6%/km² and 3.2%/km² with a mean value of about 2.4%/km². Secondary maxima were obtained in the western part of the caldera, with mean values of about 1–1.2%/km². However, the probability of vent opening was not confined to these areas and, with mean values everywhere above 0.4%/km², the possibility is widespread over the caldera. Uncertainty ranged about ±30% of the mean value, with variations from ±10% to ±50% in different areas of the caldera. The probability of vent opening in the

offshore portion of the caldera was estimated at about $25\% \pm 5\%$.

Rivalta et al. (2019) followed a different approach to better constrain the distance of the vent opening from the centre of the caldera, based on the 2D axisymmetric physical modelling of magma transport after a statistical reconstruction of the stress field in the upper crust. In a Monte Carlo simulation, the authors propagated magma dykes perpendicular to the lowest eigenvector of the stress tensor σ_3 . They assumed dyke nucleation at a random depth between 3 and 4 km, placed at the caldera centre, beneath the Rione Terra (Pozzuoli). The model considers a homogeneous tectonic stress and a uniform unloading stress applied to the caldera floor, the latter affected by an axisymmetric topography. The stress coefficients were estimated through a Bayesian technique that considered the past vent locations. The model performance was tested on the events of epoch 3 and the Monte Nuovo eruption. The radial distance of Monte Nuovo from the defined caldera centre was found to be very close to the modal value of the estimated probability distribution, at 2–3 km from the centre of the NYT caldera. The authors also evaluated the effects of a simplified non-axisymmetric topography along two 1D directions, towards northeast and south. These results were broadly consistent with previous maps and indicated a higher probability of vent opening in the north-eastern portion of the caldera.

3.2 Timing of a Future Eruption

The long-term temporal forecasting of volcanic eruptions in the CFC is particularly complex and very few studies have been devoted to its solution. Indeed, constant rates based on the ratio of number of eruptions over time turn out to be inadequate due to the strong temporal clustering occurring at various time scales. Spatial locations and temporal rates also appear to be related. Uncertainty affecting the past record cannot be neglected when the spatial and temporal clustering properties are evaluated. A spatial–

temporal model for eruption rates at the CFC was developed by Bevilacqua et al. (2016). As a first step, a probability model of the past eruptions and its uncertainty was developed, using the available radiometric ages and the known stratigraphic sequence of the events (Smith et al. 2011 and references therein). Then, a space–time doubly stochastic non-homogeneous Poisson-type model with a local self-excitation feature was defined. This model, based on the vent locations in Bevilacqua et al. (2015), was able to generate spatial–temporal clusters of eruptions statistically consistent with the CF reconstructed record (Bevilacqua 2016). Results allowed the evaluation of similarities and differences among the three epochs of activity as well as the derivation of the eruptive base rate of the caldera (i.e., excluding the clusters) and its capacity to generate clusters. Thanks to this uncertainty assessment, it was possible to obtain a temporal probability model able to describe the temporal and spatial eruptive behaviour of the caldera over the past 15 kyrs.

The results of Bevilacqua et al. (2015, 2016), including the dependence of both scale and time probability of an eruption on the vent opening location, were later revisited by Bevilacqua et al. (2017). This resulted in separate vent opening probability maps conditional on the western and eastern sectors of the subaerial portion of the caldera, and a conditional version of the vent opening map was developed. This version enabled the authors to restrict the eruption vent sampling inside various subsets of the caldera (typically of 2–4 km in diameter) and to produce PDC invasion hazard maps under such conditions (see Sect. 3.4.2 and Fig. 14a, b).

3.3 Size of a Future Eruption

A first attempt to constrain the size of a future eruption of the CFC was made by Orsi et al. (2004), who developed a dataset of the areas covered by PF and PDC deposits of the eruptions of the past 15 kyrs, as proxies of the magnitudes of the eruptions. These areas were constrained by the 10 cm isopachs for fallout beds, and the

presence of sedimentological features indicating a horizontal component in the transport of the particles for PDCs deposits. An analysis of the magnitude–frequency ratio of the PF deposits led Orsi et al. (2004) to infer that in epoch 3 the probability distribution had a polymodal profile, with one mode between 0 and 100 km², another between 100 and 500 km², and a third, represented by the A-MS outlier, at 800 km². Finally, the authors suggested that although A-MS could not be excluded as the maximum expected event, the most probable maximum event in the case of renewal of volcanism in the short- or mid-term was an eruption falling between 100 and 500 km² area for PF deposits. Very large-scale eruptions, such as the CI and NYT caldera forming events, were not included in the dataset due to their very low probability of occurrence, likely below 1% based on frequency of occurrence.

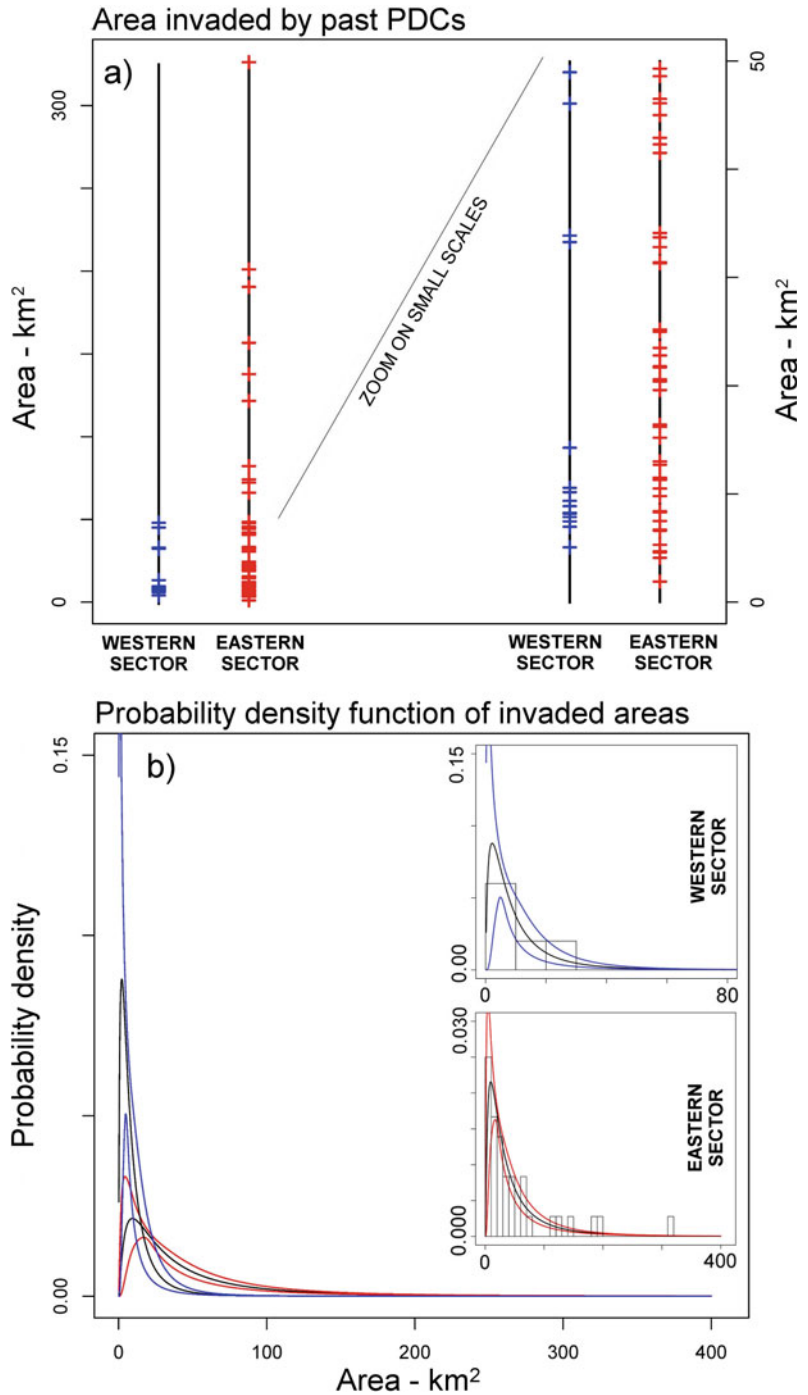
Orsi et al. (2009) built upon the above analysis by developing a quantitative long-term forecast of the size of the next eruption. Some physical parameters of 22 explosive eruptions of the CFC occurred during the past 5 kyrs were analysed. They included dispersal area, volume and density of the pyroclastic deposits, volume of erupted magma, total erupted mass, and eruption magnitude. This analysis resulted in a size classification of the explosive eruptions, which were grouped into three classes: small, medium, and large, each with a conditional probability of occurrence. They selected some reconstructed events as representative of each size class. A small-size explosive event (e.g., Monte Nuovo, Averno 2) is the most likely with a probability of about 60%; a medium-size (e.g., Astroni 6) has a probability of occurrence of about 25%; a large-size (A-MS) is the least likely with a probability of about 4%. An effusive eruption has a chance of occurrence of about 11%.

Neri et al. (2015b) designated the areas invaded by PDCs as a random variable representative of the uncertainty affecting the scale of the next eruption with the aim to quantifying the PDC hazard. This approach was based on a continuous statistics of the areas expected to be inundated by a PDC, rather than on discrete classes of the total erupted volume. Based on the available field

datasets and estimates for poorly exposed old deposits, and using alternative expert judgment procedures (Bevilacqua et al. 2015), the authors considered that a radial underestimation error of deposit boundaries (treated as a source of uncertainty) varied between about 150 and 1,000 m, with a mean value of about 500 m. Thus, they generated log-normal probability density functions of spatial extent distribution considering either the past 5 kyrs or the past 15 kyrs datasets. The presence of several intermediate data points between the main empirical distribution for the 15 kyrs dataset and the A-MS event allowed a quasi-continuous distribution of the PDC inundation areas to be hypothesised. The curves were very similar, although the one related to the longer time interval had a slightly higher number of smaller and larger events, and less medium scale events.

Bevilacqua et al. (2016) developed a probability model of the post-NYT caldera eruptions record, which included some time-volume statistics of the sum of PF and PDC deposits (see also Sect. 2.1). Uncertain volumes were uniformly sampled inside three separate intervals associated with different volumes of erupted magma (DRE): 0–0.01 km³ for very small explosive/effusive eruptions, 0.01–0.1 km³ for small explosive eruptions, and 0.1–0.3 km³ for medium explosive eruptions (similarly to Orsi et al. 2009). If volume estimates were available 5th and 95th percentiles were adopted, corresponding to ±50% relative errors (Fig. 6). The analysis included a comparison of the volumes of magma erupted in the eastern and the western sectors, showing that the latter were significantly lower. A first attempt to find a correlation between eruption size and vent location was made by Bevilacqua et al. (2017) in the framework of a more general study mainly aimed at producing PDC hazard maps. They showed that the western sector of the caldera was characterised by smaller size events, as well as by a less frequent and less clustered activity (Fig. 9). This resulted in significantly different probability distributions for the PDC sizes according to the specific sector of vent opening considered.

Fig. 9 **a** Representation of the areas invaded by pyroclastic density current originating in the western (blue) or eastern (red) sectors of the caldera. Each coloured dash represents an event. The sequence is ordered increasingly as a function of the areal extents. On the right of the plot is displayed a zoom of the small scales data. **b** Probability density functions (log-normal class) for the invasion areas originating in the western (blue) or eastern (red) sectors of the caldera. The black curve is the mean value and the coloured curves are the 5th and 95th uncertainty bounds. In the small boxes the two estimates are displayed at different scales and the histogram data are included. Figure modified after Bevilacqua et al. (2017)



3.4 Style of a Future Eruption

In addition to the previously presented definition of the size classes of the past eruptions of the

CFc and the possibility for each of them to occur in case of renewal of volcanism in short- to mid-terms, Orsi et al. (2009) also discussed the likely style of a future eruption that will be either

effusive or explosive of three different sizes. The possibility that the next eruption will be the first of a series of events following each other at short time intervals (years or tens of years), that more than one eruption will occur in the same vent area, and that two contemporaneous eruptions will occur at vents located in different portions of the NYT caldera cannot be ruled out. An effusive eruption will very likely extrude viscous magma that will generate either lava flows travelling short distances or a lava dome. An explosive eruption, regardless of its size, will likely alternate magmatic and phreatomagmatic phases that will generate particle fallout and PDCs. The detailed sequential development of the eruption dynamics and the related phenomena expected during the course of the eruption is rather difficult to predict. The areas affected by accumulation of falling pyroclastic fragments will be exposed to different effects (e.g., Wilson et al. 2014, for a review) including roofs collapse (Blong 1981, 2003; Macedonio and Costa 2012), disruption to aviation (Casadevall 1994; Folch and Sulpizio 2010), water pollution (Blong 1984; Wilson et al. 2010), damage to electric power supply and radio communication (Wilson et al. 2014), health problems to humans and animals (Baxter and Horwell 2015; Armienta et al. 2011; Flueck 2016), lahars generation and damages to agriculture (Cronin et al. 2014). Fatalities will occur in the proximal areas, through roof collapse, asphyxiation and burial (Spence et al. 2005; Brown et al. 2017). PDCs will spread either 360° from the vent or over preferential sectors. Their runout will be significantly affected by the topography surrounding the vent; higher elevations can divert the currents, valleys can channelise them. PDCs entering the sea will have the potential to produce vast clouds of water vapour bearing accretionary lapilli, and to generate tsunami waves. Due to their velocity, temperature, and particle concentrations, PDCs can produce heavy damage to urban structures and lethal conditions for human beings (Baxter et al. 2005; Neri et al. 2015a). Mele et al. (2015) reconstructed the dynamics of the PDCs generated by some phases of the Averno 2 (small scale), Astroni (intermediate scale) and A-MS (large

scale) eruptions. They combined facies architecture with laboratory analysis and physical modelling to evaluate the dynamic characteristics of the original currents. Facies analysis indicated that the deposits of the small and intermediate events resulted from pyroclastic surges fed by multiple explosions of phreatomagmatic origin. Instead, in the large-scale event some of the currents started as a concentrated flow near the vent and then evolved laterally into expanded flows by the propagation of the basal shear current. Finally, the authors provided probability density functions for the dynamic pressure and the particle volumetric concentration.

Esposti Ongaro et al. (2006) explored the effects of the presence of different amounts of CO₂ in the 4 wt% H₂O-bearing A-MS magma, by simulating the eruption dynamics from the base of the volcanic conduit up into the atmosphere. Within the range of conditions explored, the eruption style and dynamics in the atmosphere were mainly controlled by the H₂O content. Nevertheless, the partial substitution of H₂O with CO₂ in the erupted magma produced a substantially more collapsing behaviour of the resulting column.

At the lower range of the size spectrum of explosive eruptions in the CFc there are phreatic explosions, i.e., driven by over pressurised geothermal fluids, such as H₂O, CO₂ (Barberi et al. 1984; Macedonio et al. 2013). Phreatic explosions can have various scale. The most energetic can eject ballistics at kilometres distance (Neri et al. 1999; Houghton et al. 2015) and produce great amounts of fine dust of clay and other hydrothermally altered minerals, generating ‘soap-like’ wet deposits (Montanaro et al. 2016). Small convective plumes and pyroclastic surges can also be generated. They can precede a magmatic or phreatomagmatic eruption, although often they occur as isolated events (Barberi et al. 1993). Phreatic explosions produce less evident precursor signals than magmatic explosions and can unexpectedly occur in hydrothermal areas, like Solfatara-Pisciarelli in the CFc (Mayer et al. 2016).

In the following, we summarise both the evolution and the state of the art in development of PF and PDC hazards maps at the CFc.

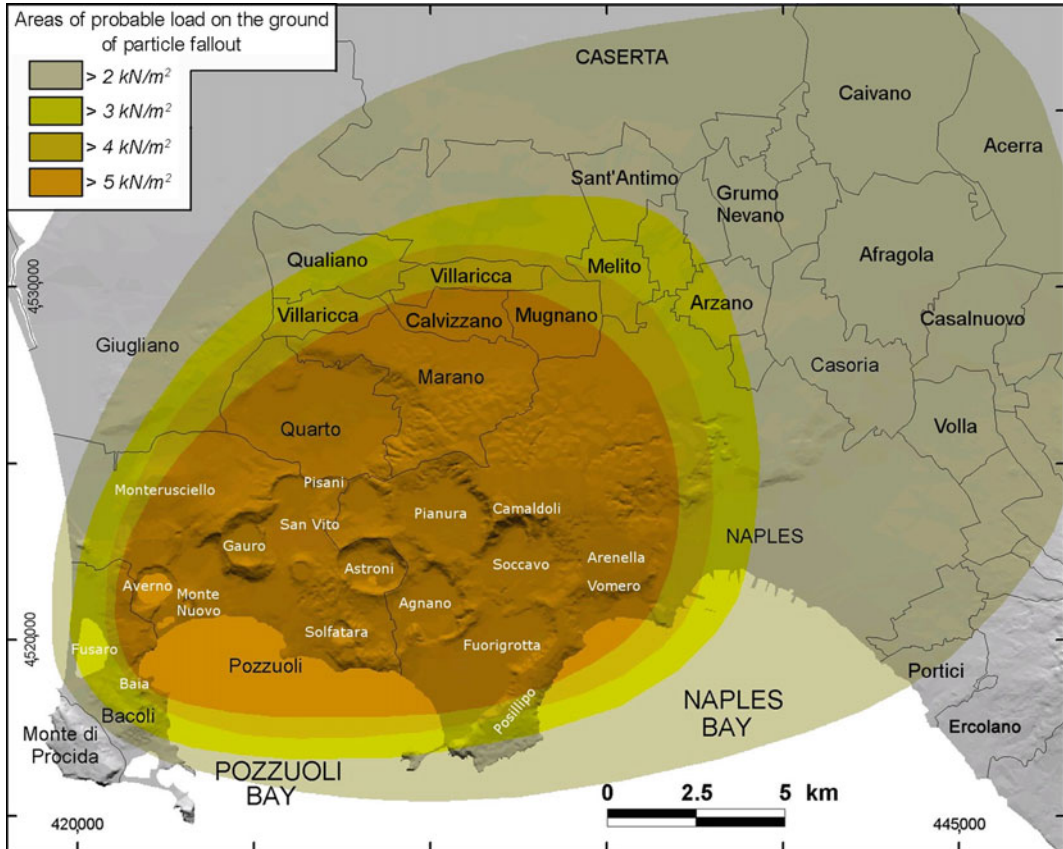


Fig. 10 Tephra fallout hazard map of the Campi Flegrei caldera. Different colours mean different tephra loads. Figure modified after Orsi et al. (2004)

3.4.1 Pyroclastic Fallout Hazard Maps

Orsi et al. (2004) constructed the first PF hazard map for the CFc (Fig. 10). The map was based on the frequency of deposition of fallout beds thicker than 10 cm (Fig. 5), their load on horizontal surfaces, and the direction of their dispersal axes. It delimits the areas that could be affected by load on the ground in excess of 2.0, 3.0, 4.0 and 5.0 kN/m^2 .

Mastrolorenzo et al. (2006, 2008) first produced PF hazard maps by using numerical modelling, for three different scenarios, and sampling empirical probability distributions of the input parameters such as column height, erupted mass, initial velocity and grain size. Average wind direction was obtained from historical data. The PF hazard level was found to depend strictly on the scenario being considered.

Orsi et al. (2009), as already reported in Sect. 3.3, evaluated the most relevant physical parameters of the 22 explosive eruptions recognised at the CFc over the past 5 kyrs. These parameters include dispersal, volume and density of the pyroclastic deposits, volume of erupted magma, total erupted mass, and eruption magnitude, and permitted to group the fallout deposits in three classes. Costa et al. (2009) simulated and analysed the PF of the three eruption scenarios of Orsi et al. (2009) using the HAZMAP computational model (Macedonio et al. 2005). This model is based on a semi-analytical solution of the two-dimensional advection–diffusion–sedimentation equation for volcanic tephra and is able to perform many simulations in a short time. The volcanological model parameters were estimated from best fit of

the model output with the field data of the eruption representative of each size class.

These parameters included total mass, eruption column height, total grain size distribution or settling velocity distribution of the particles, column shape and meteorological parameters, such as wind velocity and atmospheric diffusion coefficient. After the best-fit phase, a statistical analysis was performed by varying the meteorological conditions, namely the wind velocity profile, using a statistical set of wind profiles obtained from National Oceanic and Atmospheric Administration (NOAA) reanalysis. Probability maps, relative to the considered scenarios, were also constructed for tephra loads of 200, 300 and 400 kg/m².

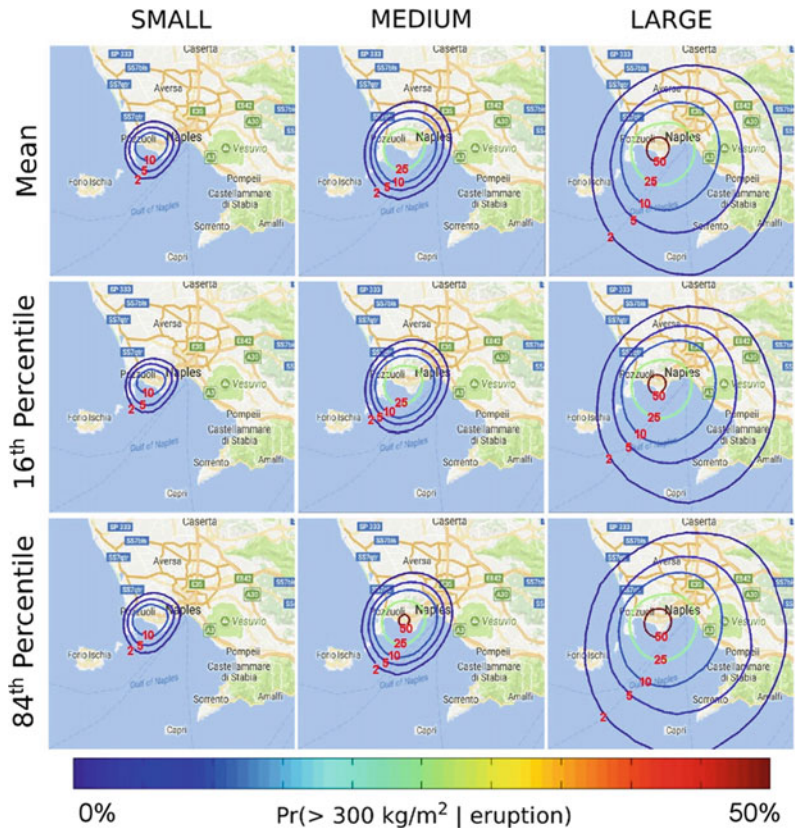
Selva et al. (2010) explored the joint effect of two great uncertainties (vent location, and eruption size) affecting PF hazards at CFC by using the tool BET_VH of Marzocchi et al. (2010). The study did not produce new simulations but relied on the data in Orsi et al. (2004) and Costa et al.

(2009). The results showed that volcanic hazard based on the weighted average of all possible eruptive scenarios is very different from the analysis of single reference scenarios.

Lirer et al. (2010) and Alberico et al. (2011) produced multi-source (CFC, Somma-Vesuvio, Ischia) PF hazard maps by combining the dispersal of past eruption products as reconstructed by field surveys and their recurrence over the whole area. They included a semi-empirical processing of the results of numerical simulation in Costa et al. (2009). Later, through numerical modelling within the BET_VH tool, a multi-source PF hazard map was obtained by Marzocchi et al. (2015b), focussing on the city of Naples. Although an underwater eruption may not generate any eruptive column, Tonini et al. (2015) focussed on the chance of PF source opening in the Pozzuoli Bay, and showed that this assumption enhances the hazard in the city of Naples.

Sandri et al. (2016) performed further uncertainty quantification on the PF hazard maps, both

Fig. 11 Conditional probability map for volcanic ash loading greater than 300 kg/m² in response to an eruption of the Campi Flegrei caldera. The contour lines, from the outer to the inner, refer to 2, 5, 10, 25 and 50%. In some panels the highest values are not reached and the corresponding curves are missing. From left to right, the hazard maps corresponding to the three different eruption scenarios (small, medium and large) are shown. The top panels report the mean values, whereas the other panels report the 16th and the 84th percentiles. Figure modified after Selva et al. (2018)



for CFc and Somma-Vesuvio volcano. The possible wind directions and speed were explored by using real winds based on model reanalysis provided by the European Centre for Medium-Range Weather Forecasts, freely available in the internet. A period of about ten years (2001–2010) was considered sufficient to obtain a robust statistical analysis (Macedonio et al. 2016). In this study, the authors first explored extra and intra-class size variability (i.e., size difference within an eruptive size class) by using a power law for the magnitude-frequency modelling. They showed that also the effects of intra-class variability within a single scenario can be relevant. Secondly, they tested both the semi-analytic 2D model HAZMAP, and the fully 3D model FALL3D (Folch et al. 2009). They found that the influence of the simulator on the statistical results is relatively small.

Selva et al. (2018) presented a state-of-the-art analysis of the hazard maps for PF at the CFc by exploring the possible eruption size, total grain size distribution of products, wind field, vent location, also accounting for their respective uncertainties. The hazard map reported in Fig. 11 is relative to a loading threshold of 300 kg/m^2 . This means that the values shown in each point represent the probability of exceeding that loading in case of eruption. Similar maps were produced for different thresholds between 1 kg/m^2 to more than $1,000 \text{ kg/m}^2$. The different hazard maps, i.e., the probability of exceeding a given loading threshold, can be successively combined with the vulnerability of the given types of roofs present in the area (e.g., Spence et al. 2005; Zuccaro et al. 2008) or used for estimating other damage such as to agriculture or those caused by secondary processes (e.g., landslides and lahars). The probabilistic hazard maps also provided the uncertainties associated with each probability. As an example, Fig. 11 reports the median, the 16th and the 84th percentiles of the probability distribution.

3.4.2 Pyroclastic Density Currents Hazard Maps

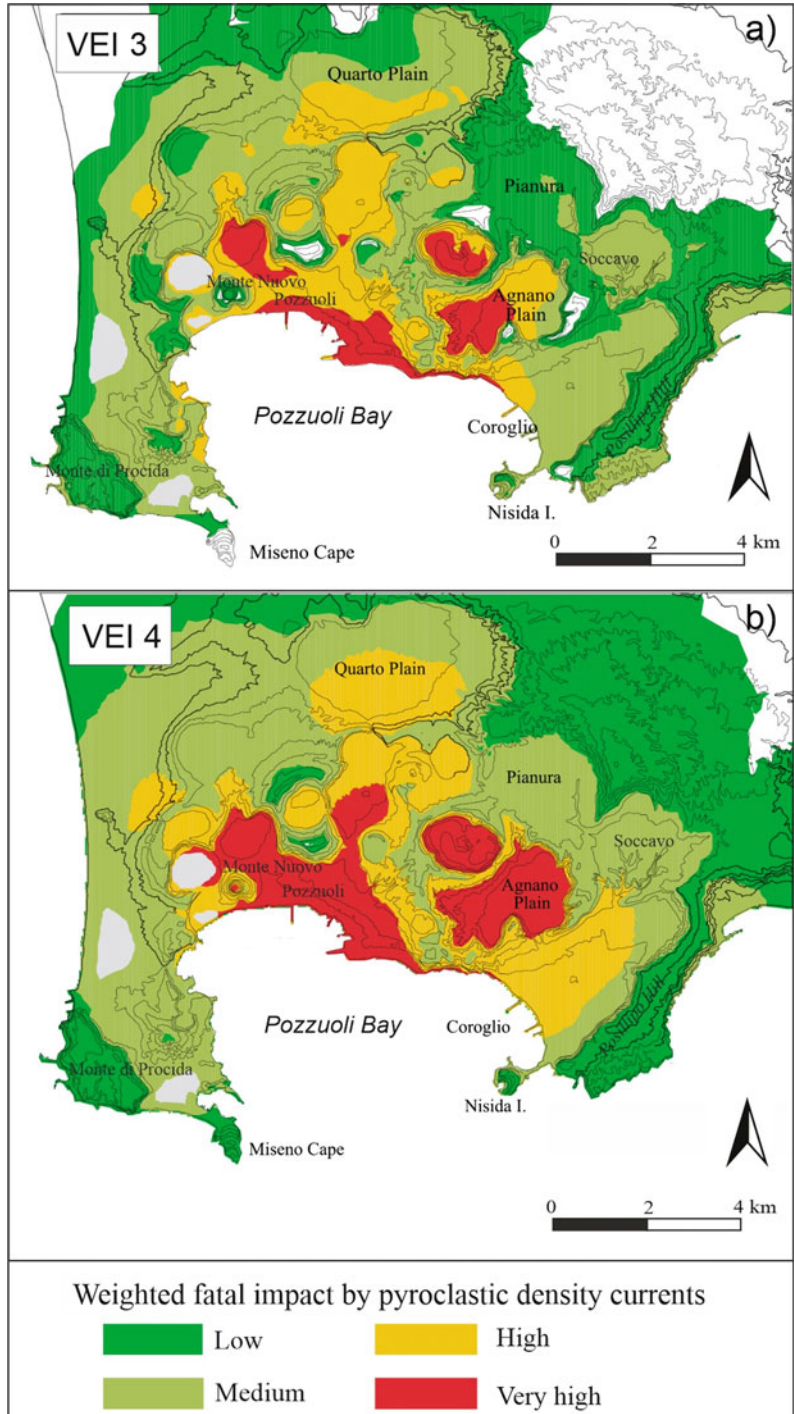
Lirer et al. (2001) provided a detailed reconstruction of the PDC deposits of six characteristic

eruptions, ranging from the Monte Nuovo small event to the Pomici Principali large event. In particular, the authors widely discussed the interaction between the flow capacity and the topography. They concluded that both Posillipo and Camaldoli hills act as effective obstacles for PDCs flowing towards the centre of the city of Naples, while Bagnoli and Fuorigrotta plains are significantly exposed to the PDC hazard.

A first qualitative PDC hazard map was developed by Alberico et al. (2002) on the basis of their vent opening map (see Sect. 3.1). They used a Monte Carlo application of the energy line model (Sheridan and Malin 1983), assuming a 6° friction angle φ , for a VEI 3 and a VEI 4 eruption with column collapse height of 100 and 300 m, respectively (Fig. 12). The resulting map for a VEI 3 eruption indicates that only limited areas have a cumulative 3% chance of being hit by PDCs erupted from a distal vent, as their propagation does not exceed a distance of 1 km. Thus, the inundation area is strongly dependent on the vent location. Instead, in case of a VEI 4 eruption, the central-eastern portion of the caldera has a 25–50% probability of being invaded by PDCs, even if they originate in other portions of the caldera. The authors also stated that a VEI 5 or higher event would inundate the whole region regardless of the vent location. Based on this study, Lirer et al. (2010) constructed multi-hazard (considering both PF and PDC) and multi-source (considering Campi Flegrei, Somma-Vesuvio, and Ischia) maps for the Neapolitan area. Later, Alberico et al. (2011) further detailed these results, focussing on the city of Naples.

Orsi et al. (2004) constructed a PDC hazard map directly based on the areal distribution and frequency of PDC deposits of the past 5 kyrs. They argued that PDCs of a future eruption would likely travel at high speed within portions of the CF lowland, defined as the area at high probability of invasion by PDCs. Some of them, depending upon vent location and energy, and in favourable morphological conditions could be able to exit this lowland towards the north and northeast, invading an area defined as the area at lower probability of invasion by PDCs.

Fig. 12 Composite probability maps of weighted fatal impact from pyroclastic flows by any eruption in any of the cells for **a** VEI 3 and **b** VEI 4 eruptions. Figure modified after Alberico et al. (2002)



Other PDC hazard maps were developed by Rossano et al. (2004) using the Monte Carlo application of a 1D physical model, while

varying 14 vent locations and 1,200 combinations of input parameters (e.g., initial velocity, density, viscosity, thickness, yield strength) of

the PDCs. The flow was assumed to be incompressible with a Newtonian or Bingham rheology, in contrast with the real dynamics of PDCs (e.g., Sulpizio et al. 2014). The input values were empirically weighted and assumed as independent. They computed the trajectories of an idealised, 1D, mass-independent flow, approximated as a material point, representing the flow plug, with an initial radial direction uniformly sampled over 360°. The results highlighted that the most mobile flows have a maximum range of ~20 km and can pass over 400-m-high topographic barriers. Otherwise, most of the flows with intermediate mobility were affected by the main topographic barriers, in particular the western slopes of the Posillipo Hill. Instead, slow-moving flows were strongly controlled by the rugged topography of the area, and stopped within few kilometres from the vent. The authors concluded that the NYT caldera floor is prone to very high inundation hazard by flows with high dynamic overpressure, whereas the centre of the city of Naples and the plain to the north of the CF have a lower probability of being affected by PDCs. Later, Mastrolorenzo et al. (2006) included these results in a multi-hazard perspective, by considering both PDC and PF hazards. This modelling approach was further detailed by Mastrolorenzo et al. (2017).

Todesco et al. (2006) performed the first 2D axisymmetric numerical simulations of PDCs generated by column collapse at the CFC, describing the transient, multiphase flow dynamics of a mixture of three solid particulate phases with different densities and dimensions in a continuous gas phase. The particulate phases were used to represent ash, pumice and lithic solid components, whereas water vapour was the only volatile component assumed in the eruptive mixture. Grain-size, density, and mass fraction of the different classes of solid particles were obtained from the analyses of the eruption deposits. The simulations provided the spatial and temporal distributions of some variables essential for PDC hazard assessment, such as flow temperature and concentration of ash in air. The simulations considered two different radial

topographic profiles representative of the south-eastern sector of the NYT caldera and accounting for different vent positions with respect to the high angle slopes bordering the Agnano Plain and the Posillipo Hill. The simulations were based upon the A-MS eruption, in particular to the magmatic phases of the eruption producing the Plinian columns that generated the B1 and D1 beds (de Vita et al. 1999). Largest events generated pyroclastic flows which were thicker and faster, and which overran topographic obstacles more easily, covering longer distances. In contrast, flows generated by small-scale events were fully confined by the distal ridge. Every time the flow decelerated, hot gases and light particles decoupled from the flow and rose to form phoenix clouds, thereby contributing to flow deceleration. As the flow propagated uphill, a portion of material segregated at the base of the flow and eventually slid back, generating back-flows that propagated toward the vent. On the other hand, the presence of two concentric obstacles reduced dynamic pressures in the distal region and prevented flow propagation in the case of small eruptions. The authors finally suggested that in the case of large events, distal obstacles as high as the Posillipo Hill could not effectively protect the area beyond, that is the centre of the city of Naples.

Then, Neri et al. (2015b) produced, through the application of a doubly stochastic approach, fully developed probabilistic maps of PDC invasion able to incorporate some of the main sources of epistemic uncertainty that influence the models. In particular, the new method combined the vent opening map of Bevilacqua et al. (2015) (Fig. 8), the density distribution of PDC invasion areas described in the previous section (Fig. 4), and a PDC integral model able to describe the dynamics of inertial dilute fully-turbulent density currents (the so-called “box-model”; Huppert and Simpson 1980). The integral model had been validated and calibrated through extensive comparison with 2D numerical simulations also on the CF topography, as detailed in Esposti Ongaro et al. (2016). It assumed that the current was vertically

homogeneous and deposited particles during propagation as a function of their (constant) sedimentation velocity. A single particle size, representative of the mean Sauter diameter of the grain-size distribution of the mixture, was adopted. Bevilacqua (2016) provided further details on the propagation model and the Monte Carlo algorithm adopted to produce the PDC hazard maps. In order to quantify the main effects of topography on the propagation of a PDC, the flow kinetic energy was compared to the potential energy associated with any topographical relief that the flow encountered (Biagioli et al. 2019). The study suggested that the entire caldera has the potential to be affected, with a mean probability of flow invasion higher than about 5% and the central-eastern area of the caldera (i.e., Agnano-Astroni-Solfatara) having invasion probabilities above about 30%, with local peaks

at or above 50% in Agnano (Fig. 13). Significant mean probabilities, up to values of ~10%, were also computed in some areas outside the caldera (i.e., over the Posillipo Hill and in some neighbourhoods of Naples). Considering the density distribution of the PDC invasion areas over the past 15 kyrs, instead of the past 5 kyrs, slightly extended the area enclosed by low-probability isolines. If the probability distribution of the PDC invasion areas excluded the occurrence of large-scale events (top 5%), the computed distribution of probability showed a general decrease in mean values of about 2%. Finally, the chance of a simultaneous activation of two separate vents during the same eruptive event was explored. Assuming that this scenario could occur in 10% of all eruption episodes, with a credible range between about 5% and 25%, the resulting mean invasion map produced slightly

Fig. 13 PDC invasion probability maps computed by assuming the vent opening distribution of Bevilacqua et al. (2015), and the spatial density distribution of invasion areas of the last 5 kyrs. The maps assume that PDCs originate from a single vent per eruption and that the vent is located in the inland part of the caldera. Contours and colours indicate the percentage probability of PDC invasion conditional on the occurrence of an explosive eruption. The maps relate to **a** the mean spatial probability, **b** the 5th percentile and **c** the 95th percentile, respectively. Figure modified after Neri et al. (2015a, b)

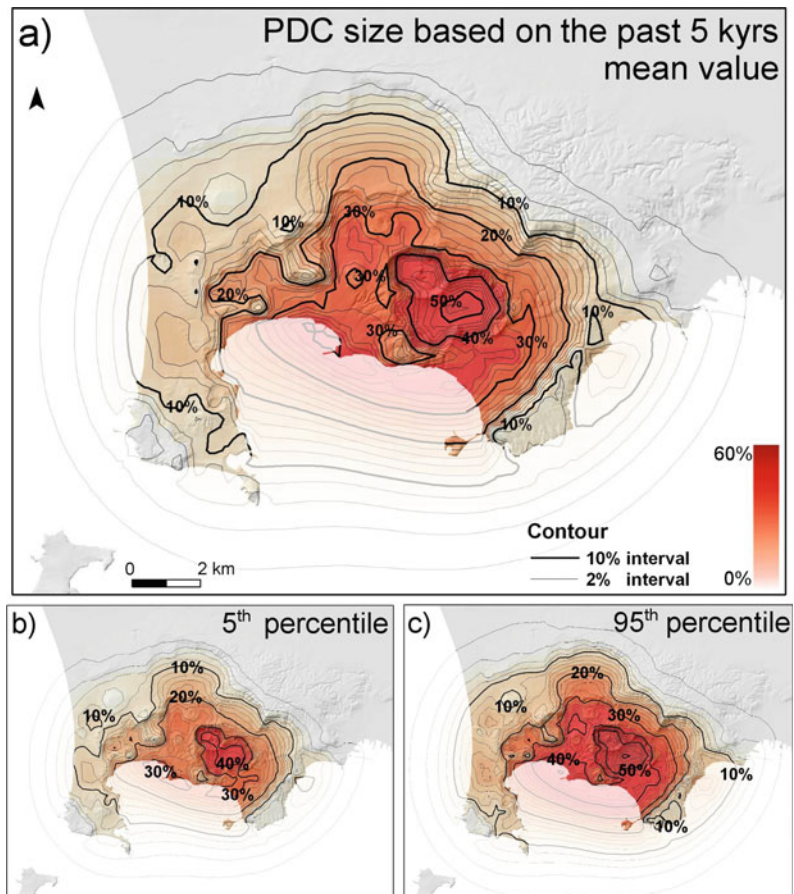
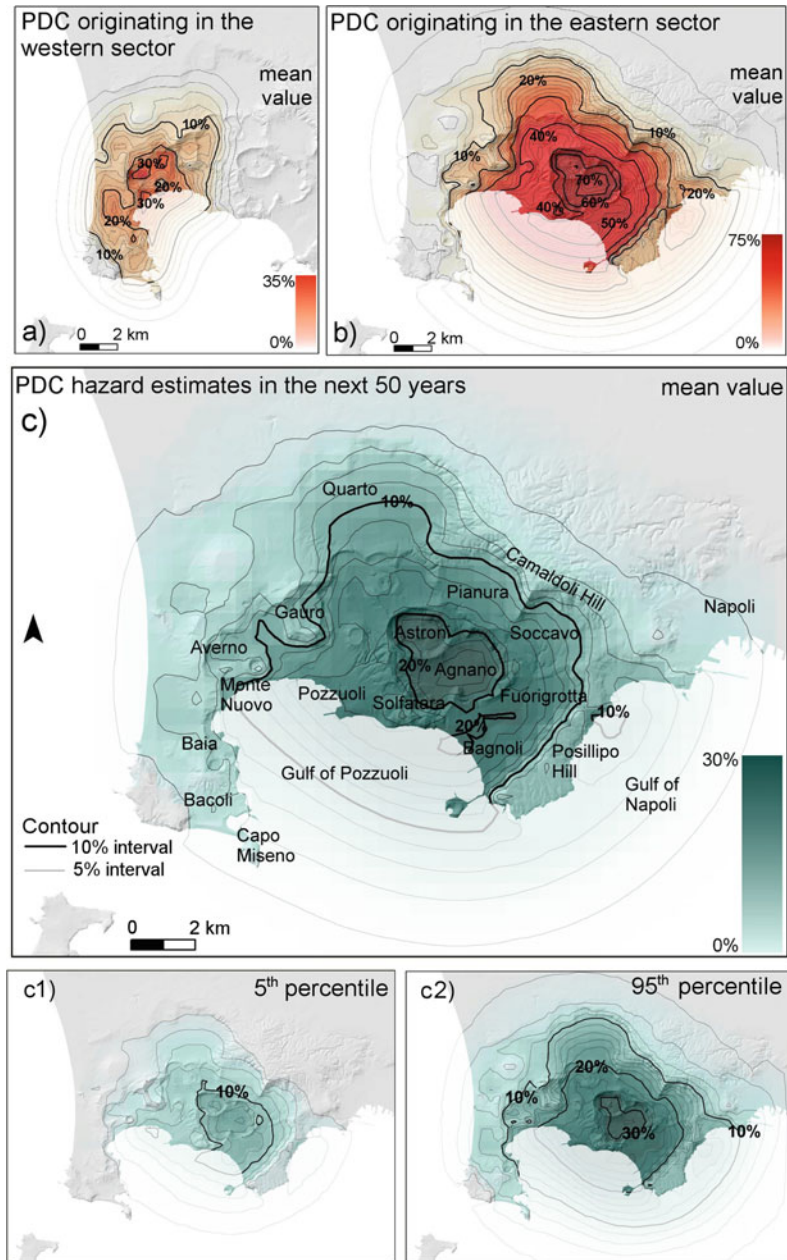


Fig. 14 PDC invasion hazard maps based on the areal size distributions and vent opening probability maps of Bevilacqua et al. (2017). Contours and colours indicate the mean percentage probability of PDC invasion conditional on the occurrence of an explosive event **a** originating inland in the western sector, **b** originating inland in the eastern sector. **c**, **c1**, **c2** show the temporal PDC invasion hazard map assuming that in AD 1538 the volcano entered a new eruptive epoch and including the possibility of a sequence of multiple events in this time period. Maps in **c1** and **c2** show the 5th and 95th uncertainty percentiles of the distribution by using the same colour scales. Figure modified after Bevilacqua et al. (2017)



wider inundation footprints with a general increase of probability values of about 2%. The uncertainty range on invasion probabilities inside the caldera typically was between ± 15 and $\pm 35\%$ of the local mean value, with an average of about $\pm 25\%$; wider uncertainties were found outside the caldera, with an average

above $\pm 50\%$ and a significantly larger variability from place to place (Fig. 13).

Tierz et al. (2016) compared eighteen PDC deposits of CFC with a statistical sample of currents modelled testing again with the energy cone model, following a similar approach to Lirer et al. (2001). In particular, the authors compared

invaded area, maximum runout, and frequency of PDC arrival. The initial height and the energy cone angle were sampled according to a truncated exponential and a uniform probability distribution, respectively. These distributions were assumed to be independent. The average initial height was obtained from models of eruptive column height, assuming that the 95th percentile of the exponential was equal to the gas thrust height. The energy cone angle range was collected from values found in literature. The authors concluded that, although the energy cone model seemed able to capture the maximum runout for several events, there were circumstances in which it struggled to accurately reproduce past PDC deposits. This was usually related to PDC that became strongly channelled despite modest topography (Aravena et al. 2020). It is worth noting that fully 3D simulations of the multiphase flow model clearly showed that column collapse height is almost irrelevant in the determination of PDCs runout and intensity (Esposti Ongaro et al. 2007, 2008, 2020; Neri et al. 2007, 2021). This observation is consistent with results of integral inertial models and fieldwork evidence (Tadini et al. 2021), but it contrasts the results of the models based on the energy-line approach.

New long-term PDC invasion hazard maps for the CFc (Fig. 14) were produced by Bevilacqua et al. (2017), based on the vent opening probability of Bevilacqua et al. (2015) (Fig. 8), the density distribution of PDC invasion areas (Fig. 9), the integral inertial PDC propagation model of Neri et al. (2015a, b), and the temporal model of Bevilacqua et al. (2016). The authors further evaluated the effects of key epistemic uncertainty sources affecting the hazard assessments. This study had several results. (i) The separate analysis of the eruptive record in the western and eastern sectors of the caldera produced a significant shift of the higher probability values toward the east, with an increase of $\sim 5\%$ of the peak probability and of $\sim 3\%$ of the chance for a PDC to overcome the NYT caldera boundary toward the city centre of Naples. Vice versa, the hazard levels were significantly reduced on the western sector of the caldera (Fig. 14a, b). (ii) Major differences were

highlighted between a map generated by considering all the scales up to a given PDC invasion area, and one generated assuming a specific PDC invasion area (i.e., conditional to the occurrence of a PDC of a given size). (iii) Given the assumption that each vent was inside one of the zones in which the CFc was subdivided, a PDC originated in the Agnano zone would have about three times more chance to overcome the Posillipo Hill than one starting in the Astroni zone. In contrast, the area subject to significant PDC invasion probability was strongly reduced when assuming a PDC originating from the Averno zone. (iv) The temporal model enabled the production of hazard maps under the assumption that in AD 1538 the volcano entered a new epoch of activity (Fig. 14c). The effect of a sequence of multiple events in the given time frame was explored. The outcomes showed that the entire caldera had a mean hazard of flow invasion above 1% in the next 10 years and above 5% in the next 50 years (although significantly larger values were estimated in the central-eastern part of the caldera, i.e., 5% and 25%, respectively). Without the assumption that the CFc in AD 1538 entered a new eruptive epoch, the hazard estimates were about three to four times lower. These results are being currently improved by using more advanced numerical models and Monte Carlo sampling techniques (Bevilacqua et al. 2019a).

The most recent attempt to construct a PDC hazard map of the CFc has been performed by Sandri et al. (2018) who developed a multi-source hazard mapping for PDC invasion over the metropolitan area of Naples. The authors considered both Campi Flegrei and Somma-Vesuvio, and accounted for both aleatory variability and epistemic uncertainty, similarly to Neri et al. (2015b) and Bevilacqua et al. (2017), but using the energy cone approach. In detail, they implemented a complete probability assessment, with a Bayesian Event Tree structure. They based the temporal rate on the model of Bevilacqua et al. (2016), but re-ran it on a reconstruction of the last 40 kyrs record. Concerning the eruption scale, the authors adopted, like Sandri et al. (2016), a power law for the total

mass erupted by explosive events, constrained with the size classes of Orsi et al. (2009). The uncertainties on column collapse height and energy cone angle were consistent with the evaluations of Tierz et al. (2016), but the authors explored various correlation structures linking the two parameters, instead of assuming them as independent variables. The authors found that the uncertainty associated with this correlation (i.e., direct or inverse) was the major source of uncertainty in their approach to produce hazard maps. According to this study, the maximum probability of PDC invasion in the next 50 years was about 7% (mean value) and ranged between 4 and 9% (assumed as 80% confidence interval), in the central-eastern part of the caldera. The mean probabilities of PDC arrival in the centre of the city of Naples were around 1% and 0.01–2%. The authors also tested the chance of arrival of a PDC originating under the sea, following a linearly decreasing probability of occurrence given an eruption, similar to Tonini et al. (2015). The obtained results showed that the changes in the probability maps were negligible.

4 Hazards Indirectly Related to Magmatism and Volcanism

In addition to the hazards directly related to volcanism, summarised in Sect. 3.4, geological and geomorphologic setting, along with the consequences of millenary human settlement (Orsi et al. 2003; Chap. [The Urban Development of Campi Flegrei, Italy](#)) expose the CFc to several hazards indirectly induced by magmatism and volcanism. The recent and ongoing short-term unrest episodes are also accompanied by seismicity as synthesised in Chaps. [The Permanent Monitoring System of the Campi Flegrei Caldera, Italy](#); [Historic Unrest of the Campi Flegrei Caldera, Italy](#); [Source Modelling from Ground Deformation and Gravity Changes at the Campi Flegrei Caldera, Italy](#). Seismicity occurs during the uplifting phases of these episodes, while is almost absent during subsidence. The higher the uplift rate, the stronger and more frequent the seismicity has been in the last

decades. The most intense detected shocks since the 1960s occurred in 1983–1984 and had maximum magnitude of 4.0–4.2 according to different estimates (Branno et al. 1984; Barberi et al. 1984; De Natale and Zollo 1986; Orsi et al. 1999; Chap. [Historic Unrest of the Campi Flegrei Caldera, Italy](#)). Their intensity reached maximum values in the Pozzuoli area, and decreased within the caldera lowland that includes the western portion of Naples, and the towns of Pozzuoli, Quarto and Bacoli.

Soft-sediment deformation is reported at various times in the history of the caldera. Orsi et al. (1992) report diapir-like deformation with intrusion of several metres of ash beds within the NYT sequence up to 15 km from Campi Flegrei. They interpreted these features as due to liquefaction of ash layers into fluid masses generated by syn-eruptive earthquakes likely associated to activation of the caldera faults. Vitale et al. (2019) reported evidence of seismically induced soft-sediment deformation in the central area of the CFc. They surveyed several soft-sediment structures including sand dikes and sand volcanoes, largely dated between 4.6 and 4.3 ka. They envisaged that the marine-transitional sands of the La Starza unit, when subject to seismic shaking, could go through liquefaction processes. The evidence of liquefaction processes increases the seismic hazard during pre-eruptive, syn-eruptive and, if any, post-eruptive phases even at a long distance from CF.

Episodes of increased unrest at calderas could be accompanied by release of great quantities of CO₂ and other toxic gases, either impulsively or for a prolonged time (Le Guern et al. 1982; Williams-Jones and Rymer 2015). Cold CO₂ is heavier than atmospheric air, and its dispersion is related to both relative temperature and weather conditions (Costa et al. 2005). In CFc, the Solfatara crater is a main source of diffuse CO₂ degassing (Chiodini et al. 2001, 2003, 2010; Caliro et al. 2007; Cardellini et al. 2017). Granieri et al. (2013) estimated that the annual emission of natural CO₂ from the Solfatara crater led to a significant air CO₂ concentration in part of the urban area of Naples, although lower than recommended health protection thresholds. The

current unrest was accompanied by a significant increase in CO₂ flux localised in Pisciarelli area (Queißer et al. 2017; Tamburello et al. 2019).

Although the case of a strong explosive scenario in deep water conditions is unlikely, the opening of an eruption vent underwater has been considered a possible event at CFc by Selva et al. (2012a) and Bevilacqua et al. (2015). Paris et al. (2019) produced a probabilistic hazard analysis of tsunami generated by subaqueous volcanic explosions related to the opening of a new eruption vent offshore. They considered a 1.5 km spaced grid of 17 different sites in the underwater part of the caldera, weighted according to the map of Selva et al. (2012a). Thus, they simulated (with a fully nonlinear Boussinesq model) the generation and propagation of the consequent tsunami waves able to reach the coasts of the Campania region for all the combinations of tsunami-generating vent sites and sizes. Results of the study showed highest hazard along the coasts of the Pozzuoli Bay that are in the imminent vicinity of the explosion centres. In a scenario with 650 m vent radius, maximum wave heights at the coast exceeded 3 m only in the Pozzuoli Bay and the eastern coast of the Procida Island. Secondary peaks of wave heights are obtained on the western coast of the Sorrento Peninsula and eastern coast of Capri Island. Instead, with a vent radius of 900 m, wave heights were in excess of 10 m, and with a vent radius of 200 m, they were 1–2 m high at most.

The excavation of many quarries adds further complexity to the geomorphic setting of the Neapolitan-Phlegraean area, with its steep caldera walls and variably preserved monogenetic volcano morphologies within a flat area inside the NYT caldera. These facilitate mass movements along slopes. A synthesis of these mass movements and relative hazard and risk is presented in Chap. [Landslide Hazard and Risk in the Campi Flegrei Caldera, Italy](#). The various types of movements depend upon the lithological characteristics of the slopes along which they occur. Falls and topples occur along slopes made up of tuffs or lavas, while slides and flows develop along slopes composed of loose pyroclastic deposits. The former two phenomena

mostly occur along the high-angle scarps of the CFc, the wave-cut cliffs of the Posillipo Hill, and the vertical walls of quarries. These gravitational movements are favoured by wind and sea erosion on highly fractured tuffs. Slides and flows mobilise the loose pyroclastic deposits mantling the high-angle slopes of the caldera walls and the flanks of both volcanic edifices and valleys. They occur during heavy rain periods and mobilise loose material blankets generally thinner than 1 m. The volume of slide material generally does not exceed few hundreds cubic metres.

5 Short-Term Assessment of Volcanic Hazard

CFc is one of the most monitored volcanoes in the world (see Chap. [The Permanent Monitoring System of the Campi Flegrei Caldera, Italy](#)), and the main monitored parameters can be divided in three groups: seismic, geodetic, geochemical. A significant uncertainty affects any forecasting effort based on the registered information, because previous pre-eruptive data for CFc to train with are very scarce. Few attempts have been made for the only historical eruption of the caldera: Guidoboni and Ciuccarelli (2011) systematically analysed historical documents; Di Vito et al. (2016) exploited the historical, archaeological and geological record to estimate the ground deformation before the eruption; Di Napoli et al. (2016) investigated the related offshore degassing. Interaction of the magmatic and hydrothermal systems complicates the interpretation of detected signals. Finally, caldera unrest may produce intense signals not followed by an eruption, and, at the same time, the final precursory signals before the eruption may be significantly weaker than those registered during the unrest phase (e.g., Newhall and Dzurisin 1988a, b; Acocella et al. 2015).

Crucial observations in the final pre-eruptive phase include the acceleration in the seismic count, and in the rate and pattern of ground deformation. The Real-time Seismic Amplitude Measurement may become particularly relevant when intense seismic activity hinders event counting.

Moreover, the detection of acid gasses like HF, HCl, SO₂ in the fumaroles, and the opening of new hydrothermal vents is an additional critical element (Caliro et al. 2014; Chap. [The Hydrothermal System of the Campi Flegrei Caldera, Italy](#)). Variation in the geometry of the deformation, such as migration of the zone of maximum uplift leading to a bimodal profile, would represent a fundamental clue of the magmatic intrusion at shallow depth, but it was never detected in the CFc (Corrado et al. 1977; Berrino et al. 1984; Orsi et al. 1999; Del Gaudio et al. 2010; De Martino et al. 2014, 2020; Bevilacqua et al. 2020a).

The temporal evolution of the system is characterised by the greatest uncertainty. Unrest signals may persist for months/years before an eruption, but clear evidence of an incoming eruption may become detectable only few days/hours before the actual event. Large-scale variations historically recorded before the AD 1538 eruption suggest decade-long unrest, with a final phase of a couple of months of strong seismicity and a rapid uplifting of the vent opening area only a few hours before the eruption onset. This extremely long and intense unrest resulted in a relatively small eruption (Guidoboni and Ciuccarelli 2011; Di Vito et al. 2016 and references therein). Evidence of fast magma mixing and ascent has been found through geochemical and isotope-geochemical investigations of the products of recent eruptions (i.e., Monte Nuovo, Astroni 6, Averno 2). The results of these studies also suggest time intervals of tens of hours to few days from injection of a new magma batch in the shallow reservoir, with related mixing, to the eruption (e.g., Rutherford 2004; Perugini et al. 2010; Chaps. [An Evolutionary Model for the Magmatic System of the Campi Flegrei Volcanic Field \(Italy\) Constrained by Petrochemical Data; Origin and Differentiation History of the Magmatic System Feeding the Campi Flegrei Volcanic Field \(Italy\) Constrained by Radiogenic and Stable Isotope Data; Rheological Properties of the Magmas Feeding the Campi Flegrei Caldera \(Italy\) and Their Influence on Mixing Processes; Magma Chamber Dynamics at the Campi Flegrei Caldera, Italy](#)).

Selva et al. (2012b) developed an event tree for the volcanic unrest of the CFc through a five-years long investigation that involved over 30 researchers, including experts in geophysical monitoring, fluid geochemistry, and in the volcanic history of the CFc. Node 1 of the tree evaluated if the caldera is in state of unrest or quiescence. Node 2 evaluated if the unrest is driven by a magmatic process. Node 3 evaluated the occurrence of a volcanic eruption in the following month. Different signals and Boolean observations were recognised to be crucial in the estimation of the probabilities at each node. Seismic signals were present in every node, the involvement of magma was recognised from the depth and waveforms of earthquakes, and the approaching of an eruption was associated with a significant acceleration in the seismic activity. Application of this event tree analysis resulted in ~40% probability of eruption in August 1983, during the major 1982–1984 unrest episode, and up to ~10% probability of eruption during the later minor uplift episodes. Currently efforts are being made for a real-time updating of vent opening maps through merging the long-term information with the short-term localisation and careful spatial-interpolation of the signals (e.g., Selva et al. 2015; Patra et al. 2019; Sandri et al. 2020).

Macedonio et al. (2014) hypothesised that the intrusion of a sill can be responsible for the dynamics observed during unrest at calderas, and developed a dynamic model of sill intrusion in a shallow volcanic environment. The model is based on the numerical solution of the equation for the elastic plate, coupled with a Navier–Stokes equation for simulating the dynamics. The stress field produced by the intrusion is mainly concentrated in a circular zone that follows the sill intrusion front (D'Auria et al. 2015; Giudicepietro et al. 2016, 2017; Chap. [Source Modelling from Ground Deformation and Gravity Changes at the Campi Flegrei Caldera, Italy](#)).

Amoruso et al. (2014a, b) interpreted the deformation history of the CFc in the periods 1980–2010 and 2011–2013 as a consequence of paired deformation sources. In particular, a

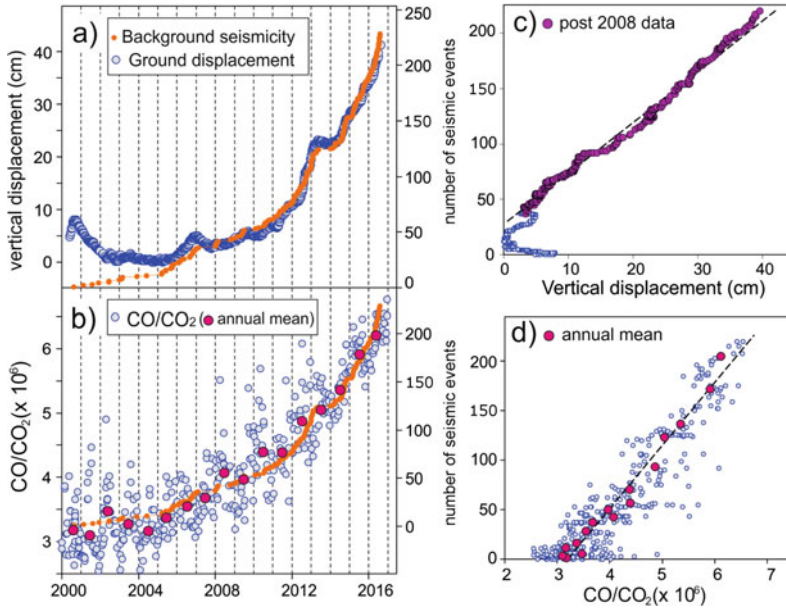


Fig. 15 Background seismicity compared with other observations. **a** Chronogram of the cumulative background seismicity (orange dots) and vertical ground displacement at the RITE GPS station at Rione Terra, Pozzuoli. **b** Chronogram of the cumulative background seismicity (orange dots) and fumarolic CO/CO₂ ratios.

c Binary plot of the cumulative background seismicity vs. the vertical ground displacement at the RITE GPS station. **d** Binary plot of the cumulative background seismicity vs. the fumarolic CO/CO₂ ratio (the magenta dots refer to annual mean values of both CO/CO₂ ratio and seismicity). Figure modified after Chiodini et al. (2017a, b)

quasi-horizontal, northwest-southeast elongated crack, embedded in an elastic layered half-space at a depth of about 3,600 m, satisfies large-scale deformation. Residual deformation is confined to the area of the Solfatara fumarolic field and satisfied by a small spheroid located at about 1,900 m depth. All source parameters but volume change are constant over time. A synthesis of the hypotheses proposed on the source of the recent short-term deformation events is presented in Chap. [Source Modelling from Ground Deformation and Gravity Changes at the Campi Flegrei Caldera, Italy](#).

In general, although uncertain until the last hours, the approach of an eruption is believed to be associated with a substantial acceleration in the unrest signals (Chiodini et al. 2016; Kilburn et al. 2017). Chiodini et al. (2017a) studied the inter-event times of the post-2000 seismicity at the CFc and distributed it into different populations. The low inter-event times population represented swarm events, while the high inter-arrival times population marked background

seismicity. The background seismicity was found to increase at the same rate of the ground uplift and of the concentration of the fumarolic gas species more sensitive to temperature (Fig. 15). The authors proposed that the whole sequence of the CFc unrest episodes since 1950 belongs to a single evolutionary trend of accumulating stress and crustal damage, and that the continuation of the trend will favour the progressive approach to eruptive conditions. After 2016 the rate of seismicity, both in terms of event count and strain release, sped up faster than the rate of ground displacement (Bevilacqua et al. 2020c). De Siena et al. (2017) studied the seismic source locations and waveform attenuation of earthquakes in the CFc during the 1983–1984 unrest episode, constraining a 4–4.5 km deep northwest-southeast striking aseismic zone of high attenuation off-shore Pozzuoli, a 3–4 km deep reservoir of supercritical fluids under Pozzuoli, and a shallower aseismic deformation source under Solfatara. They showed that the high attenuation domain controlled the largest monitored seismic,

deformation, and geochemical unrest at the caldera (Chiodini et al. 2012, 2015).

Giudicepietro et al. (2021) analysed the two episodes of seismicity and gas emission that occurred on October 7, 2015 (M_d max = 2.5) and December 6, 2019 (M_d max = 3.1) also in terms of ground displacement rates before and after the episodes. They interpreted these as examples of repeated volcanic and (or) hydrothermal system pressurisation that culminate in injection of fluids along a conduit-like path (Chiodini et al. 2017b; Giudicepietro et al. 2019) which behaves as a valve that allows fluids discharge and temporary depressurisation of the source region. The CO_2 flux from the main Pisciarelli fumarolic field has increased by a factor > 3 since 2012, reaching in 2018–2019 levels that are comparable to those typical of a medium-sized erupting arc volcano (Queißer et al. 2017; Tamburello et al. 2019).

Bevilacqua et al. (2020b) described a first assessment of the “failure time” on present-day unrest signals at the CFc based on the horizontal deformation data collected between 2011 and April 2020 at eleven GPS stations. In particular, they applied a probabilistic approach that enhanced the well-established failure forecast method of Voight (1988) by incorporating a stochastic noise in the linearised equations and a mean-reversion property to constrain it (Bevilacqua et al. 2019b). The new formulation enabled the processing of decade-long time windows of data, including the effects of variable dynamics. The “failure time” is realised when the system will reach a critical state if the accelerating trend observed in the monitoring signals will not change in the future. The possibility for false alarms is not eliminated by this method, and included in this category is the “arrested” (or failed) eruption, in which the volcano displays the precursory symptoms typical of an eruption, but does not culminate with magma reaching the surface (Cornelius and Voight 1995). This is a phenomenon typical of restless calderas (Acocella et al. 2015). Based on the assumption that the trends observed in the last several years will continue in the future, Bevilacqua et al. (2020b) provided temporal forecasts, with uncertainty quantification, of a

range of failure times (possibly indicative of eruption times). The probability density function of a failure time had peaks of about 12% mean probability per year, and 95th percentile values that can reach 25–30% probability per year (Fig. 16). The analysis of the data of the four GPS stations showing greatest displacement values produced failure time probabilities of 31–36% in 5 years, 60–64% in 10 years, 92–94% in 25 years. However, the interpretation of the failure time as the onset of a volcanic eruption is speculative in caldera systems (Kilburn 2018). Different types of signals can produce different forecasts, and the same type of signals recorded in different locations can produce different results (Bevilacqua et al. 2020c). Moreover, these results relied on long-term trends registered across multiple years. It is worth mentioning that future variations in monitoring data could either slow down the increasing trends so far observed, or speed them up. Moreover, to model any short-term trend, an appropriate time window should be selected.

6 Main Outcomes and Future Implications

The Campi Flegrei caldera (CFc) hazard assessment is complex, although the many studies carried out through time have produced some likely scenarios and probabilistic estimates in case of renewal of volcanism in short-mid-terms largely shared by the scientific community, and summarised in the following.

Astroni-Agnano-Solfatara is the most probable area in which a vent will open, while the Averno-Monte Nuovo is the second most probable one. In general, the vent could open over a region at 2–3 km from the centre of the NYT caldera, although not symmetrically distributed, but most likely occurring in its central-eastern portion. However, a significant uncertainty affects these results, and a non-negligible vent opening probability spreads over the whole caldera. Moreover, multiple vents opening at the same time cannot be ruled out. The information arising from the monitoring network will likely

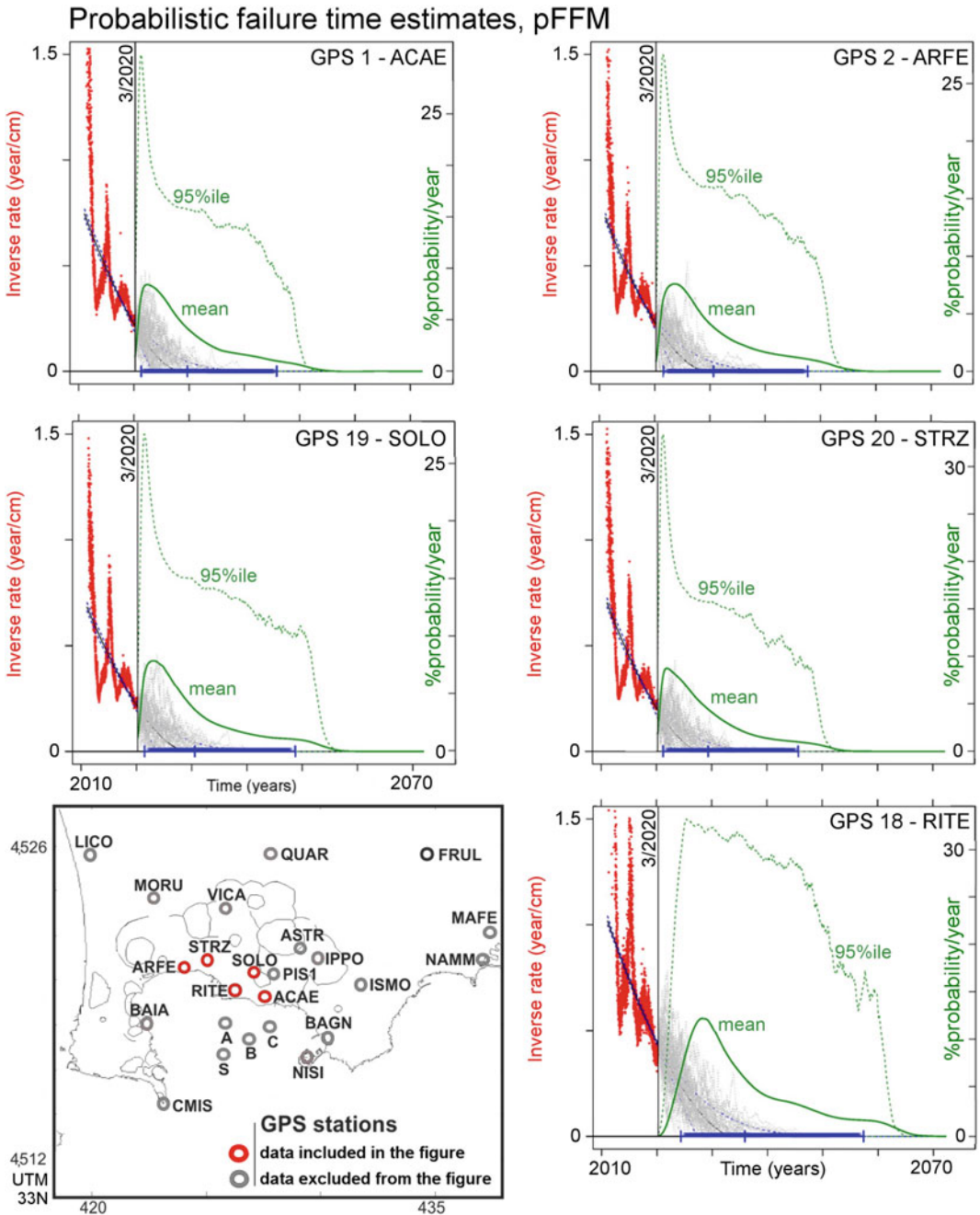


Fig. 16 Probability forecasts of the failure time of CFC using the 1/2011–3/2020 GPS data. Red points on the left are inverse-rate data. The green continuous line on the right is mean values of the annual probability of failure, dashed lines mark its 95th percentile values. A blue line

bounds the 90% confidence interval of the forecast. Grey dotted lines display 50 stochastic solution paths. The GPS stations are mapped in the lower left corner (UTM 33 T coordinates). Figure modified after Bevilacqua et al. (2020b)

constrain the vent opening location to a specific area, although it is not possible to foresee how long before the eruption onset.

The eruptions of the CFc, excluding the caldera-forming events, have ejected volumes of magma up to 1 km³ DRE. However, only four over a total of seventy events have been large eruptions, and the probability that the next eruption will be of medium or smaller size (i.e., < 0.1 km³ volume of magma DRE) is ~95%. Larger size and more frequent eruptions tend to be localised in the central-eastern portion of the NYT caldera. The inter-event times of volcanic eruptions span from a few years to thousands of years between two subsequent epochs of activity. Inside the epochs, the mean recurrence time is tens of years, but their time sequence is not Poissonian and temporal clusters are evident. However, once these clusters are considered and modelled, the system appears to have followed a self-consistent behaviour in the last 15 kyrs with the eruptions of the past 5 kyrs as a representative sample of all those occurred after 15 ka.

The next eruption can be either effusive or, more likely, explosive, and the hazards that it will generate depend upon its style. An effusive eruption could produce extrusion of a lava dome and/or lava flows. An explosive eruption could be in the range from a phreatic to a Plinian event. The most expected hazards from renewal of explosive volcanism at CFc, corresponding to those with the highest impact on environment and humans, are therefore PF and PDCs. It is worth noting that the winds blow more frequently from west to east, with a more pronounced effect shown by the stratospheric winds above 10–11 km. This means that a volcanic eruption will have higher probability to produce a deposit towards east and this probability depends on the column height. PF deposits in excess of 300 kg/m² can affect most of the caldera and the city of Naples with more than 10% probability, as well as the territory that extends for tens of kilometres to the northeast of the CFc, with more than 1% probability, given an eruption.

The entire caldera has the potential to be affected by PDC invasion with mean probability above ~30% in the central-eastern, and above ~50% in Agnano area. However, the high-angle slopes of the caldera morphological boundary tend to act as barriers for small PDC. Nevertheless, these barriers can be overcome in case of large PDC and/or if the eruptive vent lies close to the caldera boundary. Thus, invasion probabilities of ~5–10% have been estimated for the urbanised areas along the eastern slopes of the Posillipo Hill.

In conclusion, probability hazard assessment is particularly complex for CFc due to the sparse location of potential vents and the large variability of eruption styles and sizes that cannot be, at the present time, effectively constrained by monitoring signals. CFc may persist in state of unrest for a long time (decades?), periodically displaying precursor signals that would likely lead a central volcano to eruption. At the same time the possibility of an eruption, with clear pre-eruptive signals only occurring short before the event cannot be ruled out. Nevertheless, volcano monitoring may likely improve the estimates of the probability of vent opening and weather forecasts can constrain the wind field in the near future. From this point of view, the PF and the PDC hazard maps should be regarded as a dynamical tool to be used by decision makers for both long-term land-use zoning of volcanic areas and short-term risk analysis, such as managing volcano crises. These reasons increase the importance of having a robust and flexible hazard model based on the past behaviour of the volcano as well as on all other monitoring and modelling information.

Large part of the analyses and thematic maps presented in this chapter have been used, together with vulnerability and socio-economical information, by the Italian Civil Protection Department of the Presidency of the Council of Ministers for the evaluation of risk scenarios and the elaboration of the National Emergency Plan of the CFc (www.protezionecivile.it).

Acknowledgements Valerio Acocella and Greg Valentine are gratefully thanked for reviewing a first version of the manuscript.

References

- Acocella V (2010) Evaluating fracture patterns within a resurgent caldera: Campi Flegrei, Italy. *Bull Volcanol* 72:623–638. <https://doi.org/10.1007/s00445-010-0347-x>
- Acocella V, Di Lorenzo R, Newhall C, Scandone R (2015) An overview of recent (1988 to 2014) caldera unrest: Knowledge and perspectives. *Rev Geophys* 53:896–955. <https://doi.org/10.1002/2015RG000492>
- Alberico I, Lirer L, Petrosino P, Scandone R (2002) A methodology for the evaluation of long-term volcanic risk from pyroclastic flows in Campi Flegrei (Italy). *J Volcanol Geotherm Res* 116(1–2):63–78. [https://doi.org/10.1016/S0377-0273\(02\)00211-1](https://doi.org/10.1016/S0377-0273(02)00211-1)
- Alberico I, Petrosino P, Lirer L (2011) Volcanic hazard and risk assessment in a multi-source volcanic area: the example of Napoli city (Southern Italy). *Nat Hazard Earth Syst* 11:1057–1070. <https://doi.org/10.5194/nhess-11-1057-2011>
- Albert PG, Giaccio B, Isaia R, Costa A, Niespolo EM, Nomade S, Pereira A, Renne PR, Hinchliffe A, Mark DF, Brown RJ, Smith VC (2019) Evidence for a large-magnitude eruption from Campi Flegrei caldera (Italy) at 29 ka. *Geology* 47:1–5. <https://doi.org/10.1130/G45805.1>
- Amoruso A, Crescentini L, Sabbetta I (2014a) Paired deformation sources of the Campi Flegrei caldera (Italy) required by recent (1980–2010) deformation history. *J Geophys Res* 119:858–879. <https://doi.org/10.1002/2013JB010392>
- Amoruso A, Crescentini L, Sabbetta I, De Martino P, Obrizzo F, Tammaro U (2014b) Clues to the cause of the 2011–2013 Campi Flegrei caldera unrest, Italy, from continuous GPS data. *Geophys Res Lett* 41:3081–3088. <https://doi.org/10.1002/2014GL059539>
- Aravena A, Cioni R, Bevilacqua A, de' Michieli Vitturi M, Esposti Ongaro T, Neri A (2020) Tree-branching based enhancement of kinetic energy models for reproducing channelization processes of pyroclastic density currents. *J Geophys Res Solid Earth* 125:e2019JB019271. <https://doi.org/10.1029/2019JB019271>
- Armienta MA, De la Cruz-Reyna S, Cruz O, Cenicerros N, Aguayo A, Marin M (2011) Fluoride in ash leachates: environmental implications at Popocatepetl volcano, central Mexico. *Nat Haz Earth Syst Sci* 11:1949–1956. <https://doi.org/10.5194/nhess-11-1949-2011>
- Aspinall W, Blong R (2015) Volcanic risk assessment. In: Sigurdsson H, Houghton B, McNutt S, Rymer H, Stix J (eds) *Encyclopaedia of Volcanoes*, 2nd ed. Academic Press, San Diego (CA), pp 1215–1230. <https://doi.org/10.1016/B978-0-12-385938-9.00070-5>
- Aspinall WP, Cooke RM (2013) Quantifying scientific uncertainty from expert judgement elicitation. In: Rougier J, Sparks RSJ, Hill LJ (eds) *Risk and uncertainty assessment for natural hazards*. Cambridge University Press, New York, pp 64–99. www.cambridge.org/9781107006195
- Aspinall WP, Woo G, Voight B, Baxter PJ (2003) Evidence-based volcanology: Application to eruption crises. *J Volcanol Geotherm Res* 128:273–285. [https://doi.org/10.1016/S0377-0273\(03\)00260-9](https://doi.org/10.1016/S0377-0273(03)00260-9)
- Banks GN, Tilling RI, Harlow DH, Ewert JW (1989) Volcano monitoring and short-term forecasts. In: Tilling RI (ed) *Volcanic hazards: short course in geology*, vol. 1. Am Geophys Un, Washington (DC), pp 51–80. <https://doi.org/10.1029/SC001p0051>
- Barberi F, Innocenti F, Lirer L, Munno R, Pescatore T, Santacroce R (1978) The Campanian Ignimbrite: a major prehistoric eruption in the Neapolitan area (Italy). *Bull Volcanol* 41:10–31. <https://doi.org/10.1007/BF02597680>
- Barberi F, Corrado G, Innocenti F, Luongo G (1984) Phlegraean Fields 1982–1984: Brief chronicle of a volcano emergency in a densely populated area. *Bull Volcanol* 47:175–185. <https://doi.org/10.1007/BF01961547>
- Barberi F, Bertagnini A, Landi P, Principe C (1993) A review on phreatic eruptions and their precursors. *J Volcanol Geotherm Res* 52:231–246
- Baxter PJ, Horwell CJ (2015) Impacts of eruptions on human health. In: Sigurdsson H, Houghton B, McNutt S, Rymer H, Stix J (eds) *Encyclopedia of volcanoes*, 2nd ed. Academic Press, San Diego (CA), pp 1035–1047. <https://doi.org/10.1016/B978-0-12-385938-9.00060-2>
- Baxter PJ, Boyd R, Cole P, Neri A, Spence R, Zuccaro G (2005) The impacts of pyroclastic surges on buildings at the eruption of the Soufriere Hills Volcano, Montserrat. *Bull Volcanol* 67:292–313. <https://doi.org/10.1007/s00445-004-0365-7>
- Berrino G, Corrado G, Luongo G, Toro B (1984) Ground deformation and gravity changes accompanying the 1982 Pozzuoli uplift. *Bull Volcanol* 47:187–200. <https://doi.org/10.1007/BF01961548>
- Bevilacqua A (2016) Doubly stochastic models for volcanic hazard assessment at Campi Flegrei caldera. Theses, 21, Edizioni della Normale, Birkhäuser/Springer, Pisa, Italy, 227 pp. <https://doi.org/10.1007/978-88-7642-577-6>. ISBN 978–88–7642–577–6
- Bevilacqua A, Isaia R, Neri A, Vitale S, Aspinall WP, Bisson M, Flandoli F, Baxter PJ, Bertagnini A, Esposti Ongaro T, Iannuzzi E, Pistolesi M, Rosi M (2015) Quantifying volcanic hazard at Campi Flegrei caldera (Italy) with uncertainty assessment: I. Vent opening maps. *J Geophys Res* 120:2309–2329. <https://doi.org/10.1002/2014JB011775>
- Bevilacqua A, Flandoli F, Neri A, Isaia R, Vitale S (2016) Temporal models for the episodic volcanism of Campi Flegrei caldera (Italy) with uncertainty quantification. *J Geophys Res* 121:7821–7845. <https://doi.org/10.1002/2016JB013171>
- Bevilacqua A, Neri A, Bisson M, Esposti Ongaro T, Flandoli F, Isaia R, Rosi M, Vitale S (2017) The effects of vent location, event scale, and time forecasts on pyroclastic density current hazard maps at Campi

- Flegrei caldera (Italy). *Front Earth Sc-Switz* 5:72. <https://doi.org/10.3389/feart.2017.00072>
- Bevilacqua A, de' Michieli Vitturi M, Esposti Ongaro T, Neri A (2019a) Enhancing the uncertainty quantification of pyroclastic density current dynamics in the Campi Flegrei caldera. Workshop on Frontiers of Uncertainty Quantification in Fluid Dynamic FrontUQ19, 11–13 September 2019, Pisa, Italy. <http://hdl.handle.net/2122/13832>
- Bevilacqua A, Pitman EB, Patra A, Neri A, Bursik M, Voight B (2019b) Probabilistic enhancement of the Failure Forecast Method using a stochastic differential equation and application to volcanic eruption forecasts. *Front Earth Sc-Switz* 7:135. <https://doi.org/10.3389/feart.2019.00135>
- Bevilacqua A, Neri A, De Martino P, Isaia R, Novelino A, Tramparulo F, Vitale S (2020a) Radial interpolation of GPS and leveling data of ground deformation in a resurgent caldera: application to Campi Flegrei (Italy). *J Geodyn* 94(2):24. <https://doi.org/10.1007/s00190-020-01355-x>
- Bevilacqua A, Patra A, Pitman EB, Bursik M, De Martino P, Giudicepietro F, Macedonio G, Vitale S, Flandoli F, Voight B, Neri A (2020b) Utilizzo preliminare del failure forecast method sui dati GPS di spostamento orizzontale registrati nella caldera dei Campi Flegrei dal 2011 al 2020. *Misc INGV* 57:135–139. doi:<https://doi.org/10.13127/misc/57/25>. ArXiv 2007.02756 (English version)
- Bevilacqua A, Patra A, Pitman EB, Bursik M, Neri A, Voight B, Flandoli F, De Martino P, Giudicepietro F, Ricciolino P, Macedonio G, Vitale S (2020c) The Failure Forecast Method applied to the GPS and seismic data collected in the Campi Flegrei caldera (Italy) in 2011–2020, AGU Fall Meeting 2020, Abstract V029–07, San Francisco (CA). USA. <https://doi.org/10.1002/essoar.10505832.1>
- Biagioli G, Bevilacqua A, Esposti Ongaro T, de' Michieli Vitturi M (2019) PyBox: a Python tool for simulating the kinematics of Pyroclastic density currents with the box-model approach reference and user's guide. Zenodo web platform, https://zenodo.org/record/2616551#.YGbw7T_OOUk. <https://doi.org/10.5281/zenodo.2616551>
- Blong RJ (1981) Some effects of tephra falls on buildings. In: Self S, Sparks R (eds) *Tephra studies*. D. Reidel Publ Co, pp 405–420. <https://doi.org/10.1007/978-94-009-8537-727>
- Blong RJ (1984) *Volcanic Hazards: a Sourcebook of the Effects of Eruptions*. Academic Press, Sydney, Australia, 424 pp, ISBN:9781483288208
- Blong RJ (2003) Building damage in Rabaul, Papua New Guinea, 1994. *Bull Volcanol* 65:43–54. <https://doi.org/10.1007/s00445-002-0238-x>
- Branno A, Esposito EGI, Luongo G, Marturano A, Porfido S, Rinaldis V (1984) The October 4th, 1983—Magnitude 4 earthquake in Phlegraean Fields: Macroseismic survey. *Bull Volcanol* 47:233–238. <https://doi.org/10.1007/BF01961553>
- Brown SK, Croweller HS, Sparks RSJ, Cottrell E, Deligne NI, Guerrero NO, Hobbs L, Kiyosugi K, Loughlin SC, Siebert L, Takarada S (2014) Characterisation of the Quaternary eruption record: analysis of the Large Magnitude Explosive Volcanic Eruptions (LaMEVE) database. *J Appl Volcanol* 3:5. <https://doi.org/10.1186/2191-5040-3-5>
- Brown SK, Jenkins SF, Sparks RSJ, Odbert H, Auken MR (2017) Volcanic fatalities database: analysis of volcanic threat with distance and victim classification. *J Appl Volcanol* 6:15. <https://doi.org/10.1186/s13617-017-0067-4>
- Caliro S, Chiodini G, Moretti R, Avino R, Granieri D, Russo M, Fiebig J (2007) The origin of the fumaroles of La Solfatara (Campi Flegrei, South Italy). *Geochim Cosmochim Acta* 71(12):3040–3055. <https://doi.org/10.1016/j.gca.2007.04.007>
- Caliro S, Chiodini G, Paonita A (2014) Geochemical evidences of magma dynamics at Campi Flegrei (Italy). *Geochim Cosmochim Acta* 132:1–15. <https://doi.org/10.1016/j.gca.2014.01.021>
- Capuano P, Russo G, Civetta L, Orsi G, D'Antonio M, Moretti R (2013) The Campi Flegrei caldera structure imaged by 3-D inversion of gravity data. *Geochem Geophys Geosyst* 14:4681–4697. <https://doi.org/10.1002/ggge.20276>
- Cardellini C, Chiodini G, Frondini F, Avino R, Bagnato E, Caliro S, Lelli M, Rosiello A (2017) Monitoring diffuse volcanic degassing during volcanic unrests: the case of Campi Flegrei (Italy). *Sci Rep* 7:6757. <https://doi.org/10.1038/s41598-017-06941-2>
- Casadevall TJ (1994) The 1989–1990 eruption of Redoubt Volcano, Alaska: impacts on aircraft operations. *J Volcanol Geotherm Res* 62:301–316. [https://doi.org/10.1016/0377-0273\(94\)90038-8](https://doi.org/10.1016/0377-0273(94)90038-8)
- Chiodini G, Frondini F, Cardellini C, Granieri D, Marini L, Ventura G (2001) CO₂ degassing and energy release at Solfatara volcano, Campi Flegrei, Italy. *J Geophys Res* 106(B8):16213–16221. <https://doi.org/10.1029/2001JB000246>
- Chiodini G, Todesco M, Caliro S, Del Gaudio C, Macedonio G, Russo M (2003) Magma degassing as a trigger of bradyseismic events: The case of Phlegraean Fields (Italy). *Geophys Res Lett* 30:1434. <https://doi.org/10.1029/2002GL016790.8>
- Chiodini G, Caliro S, Cardellini C, Granieri D, Avino R, Baldini A, Donnini M, Minopoli C (2010) Long-term variations of the Campi Flegrei, Italy, volcanic system as revealed by the monitoring of hydrothermal activity. *J Geophys Res* 115:B03205. <https://doi.org/10.1029/2008JB006258>
- Chiodini G, Caliro S, De Martino P, Avino F, Gherardi F (2012) Early signals of new volcanic unrest at Campi Flegrei caldera? Insights from geochemical data and physical simulations. *Geology* 40(10):943–946. <https://doi.org/10.1130/G33251.1>
- Chiodini G, Vandemeulebrouck J, Caliro S, D'Auria L, De Martino P, Mangiacapra A, Petrillo Z (2015) Evidence of thermal-driven processes triggering the

- 2005–2014 unrest at Campi Flegrei caldera. *Earth Planet Sci Lett* 414:58–67. <https://doi.org/10.1016/j.epsl.2015.01.012>
- Chiodini G, Paonita A, Aiuppa A, Costa A, Caliro S, De Martino P, Acocella V, Vandemeulebrouck J (2016) Magmas near the critical degassing pressure drive volcanic unrest towards a critical state. *Nat Commun* 7:1–9. <https://doi.org/10.1038/ncomms13712>
- Chiodini G, Selva J, Del Pezzo E, Marsan D, De Siena L, D’Auria L, Bianco F, Caliro S, De Martino P, Ricciolino P, Petrillo Z (2017a) Clues on the origin of post-2000 earthquakes at Campi Flegrei caldera (Italy). *Sci Rep* 4472:2045–2322. <https://doi.org/10.1038/s41598-017-04845-9>
- Chiodini G, Giudicepietro F, Vandemeulebrouck J, Aiuppa A, Caliro S, De Cesare W, Tamburello G, Avino R, Orazi M, D’Auria L (2017b) Fumarolic tremor and geochemical signals during a volcanic unrest. *Geology* 45(12):1131–1134. <https://doi.org/10.1130/G39447.1>
- Cinque A, Rolandi G, Zamparelli V (1985) L’estensione dei depositi marini olocenici nei Campi Flegrei in relazione alla vulcano-tettonica. *Boll Soc Geol Ital* 104(2):327–348. ISSN 0037–8763
- Civetta L, Orsi G, Pappalardo L, Fisher RV, Heiken GH, Ort M (1997) Geochemical zoning, mixing, eruptive dynamics and depositional processes—the Campanian Ignimbrite, Campi Flegrei, Italy. *J Volcanol Geotherm Res* 75:183–219. [https://doi.org/10.1016/S0377-0273\(96\)00027-3](https://doi.org/10.1016/S0377-0273(96)00027-3)
- Connor C, Bebbington M, Marzocchi W (2015) Probabilistic volcanic hazard assessment. In: Sigurdsson H, Houghton B, McNutt SR, Rymer H, Stix J (eds) *Encyclopedia of Volcanoes*, 2nd ed. Academic Press, San Diego (CA), USA, pp 897–910. <https://doi.org/10.1016/B978-0-12-385938-9.00051-1>
- Cornelius R, Voight B (1995) Graphical and PC-software analysis of volcano eruption precursors according to the Material Failure Forecast Method (FFM). *J Volcanol Geotherm Res* 64:295–320. [https://doi.org/10.1016/0377-0273\(94\)00078-U](https://doi.org/10.1016/0377-0273(94)00078-U)
- Corrado G, Guerra I, Lo Bascio A, Luongo G, Rampoldi R (1977) Inflation and microearthquake activity of phlegraean fields, Italy. *Bull Volcanol* 40:169–188. <https://doi.org/10.1007/BF02596998>
- Costa A, Macedonio G, Chiodini G (2005) Numerical model of gas dispersion emitted from volcanic sources. *Ann Geophys* 48(4–5):805–815. <https://doi.org/10.4401/ag-3236>
- Costa A, Dell’Erba F, Di Vito MA, Isaia R, Macedonio G, Orsi G, Pfeiffer T (2009) Tephra fallout hazard assessment at the Campi Flegrei caldera (Italy). *Bull Volcanol* 71:259–273. <https://doi.org/10.1007/s00445-008-0220-3>
- Cronin SJ, Stewart C, Zernack AV, Brenna M, Procter JN, Pardo N, Christenson B, Wilson T, Stewart RB, Irwin M (2014) Volcanic ash leachate compositions and assessment of health and agricultural hazards from 2012 hydrothermal eruptions, Tongariro, New Zealand. *J Volcanol Geotherm Res* 286:233–247. <https://doi.org/10.1016/j.jvolgeores.2014.07.002>
- D’Auria L, Pepe S, Castaldo R, Giudicepietro F, Macedonio G, Ricciolino P, Tizzani P, Casu F, Lanari R, Manzo M, Martini M, Sansosti E, Zinno I (2015) Magma injection beneath the urban area of Naples: a new mechanism for the 2012–2013 volcanic unrest at Campi Flegrei caldera. *Sci Rep* 5:13100. <https://doi.org/10.1038/srep13100.2015>
- de Vita S, Orsi G, Civetta L, Carandente A, D’Antonio M, Di Cesare T, Di Vito M, Fisher RV, Isaia R, Marotta E, Ort M, Pappalardo L, Piochi M, Southon J (1999) The Agnano-Monte Spina eruption (4.1 ka) in the resurgent, nested Campi Flegrei caldera (Italy). *J Volcanol Geotherm Res* 91:269–301. [https://doi.org/10.1016/S0377-0273\(99\)00039-6](https://doi.org/10.1016/S0377-0273(99)00039-6)
- De Natale G, Zollo A (1986) Statistical analysis and clustering features of the Phlegraean Fields earthquake sequence (May 1983–May 1984). *Bull Seism Soc Am* 76(3):801–814
- De Martino P, Tammaro U, Obrizzo F (2014) GPS time series at Campi Flegrei caldera (2000–2013). *Ann Geophys* 57(2):S0213. <https://doi.org/10.4401/ag-6431>
- De Martino P, Guardato S, Donnarumma GP, Dolce M, Trombetti T, Chierici F, Macedonio G, Beranzoli L, Iannaccone G (2020) Four years of continuous seafloor displacement measurements in the Campi Flegrei caldera. *Front Earth Sc-Switz* 8:615178. <https://doi.org/10.3389/feart.2020.615178>
- De Siena L, Chiodini G, Vilardo G, Del Pezzo E, Castellano M, Colombelli S, Tisato N, Ventura G (2017) Source and dynamics of a volcanic caldera unrest: Campi Flegrei, 1983–84. *Sci Rep* 7:8099. <https://doi.org/10.1038/s41598-017-08192-7>
- Deino AL, Orsi G, Piochi M, de Vita S (2004) The age of the Neapolitan Yellow Tuff caldera-forming eruption (Campi Flegrei caldera—Italy) assessed by ⁴⁰Ar/³⁹Ar dating method. *J Volcanol Geotherm Res* 133:157–170. [https://doi.org/10.1016/S0377-0273\(03\)00396-2](https://doi.org/10.1016/S0377-0273(03)00396-2)
- Del Gaudio C, Aquino I, Ricciardi GP, Ricco C, Scandone R (2010) Unrest episodes at Campi Flegrei: a reconstruction of vertical ground movements during 1905–2009. *J Volcanol Geotherm Res* 195:48–56. <https://doi.org/10.1016/j.jvolgeores.2010.05.014>
- Dellino P, Isaia R, La Volpe L, Orsi G (2004) Interaction between particles transported by fallout and surge in the deposits of the Agnano-Monte Spina eruption (Campi Flegrei, Southern Italy). *J Volcanol Geotherm Res* 133(1–4):193–210. [https://doi.org/10.1016/S0377-0273\(03\)00398-6](https://doi.org/10.1016/S0377-0273(03)00398-6)
- Dempsey DE, Cronin SJ, Mei S, Kempa-Liehr AW (2020) Automatic precursor recognition and real-time forecasting of sudden explosive volcanic eruptions at Whakaari. *New Zealand. Nat Commun* 11:3562. <https://doi.org/10.1038/s41467-020-17375-2>
- Di Napoli R, Aiuppa A, Sulli A, Caliro S, Chiodini G, Acocella V, Cirao G, Di Vito MA, Interbartolo F, Nasello C, Valenza M (2016) Hydrothermal fluid

- venting in the offshore sector of Campi Flegrei caldera: A geochemical, geophysical and volcanological study. *Geochem Geophys Geosyst* 17:4153–4178. <https://doi.org/10.1002/2016GC006494>
- Di Renzo V, Arienzo I, Civetta L, D'Antonio M, Tonarini S, Di Vito MA, Orsi G (2011) The magmatic feeding system of the Campi Flegrei caldera: architecture and temporal evolution. *Chem Geol* 281:227–241
- Di Vito MA, Isaia R, Orsi G, Southon J, de Vita S, D'Antonio M, Pappalardo L, Piochi M (1999) Volcanic and deformation history of the Campi Flegrei caldera in the past 12 ka. *J Volcanol Geotherm Res* 91:221–246. [https://doi.org/10.1016/S0377-0273\(99\)00037-2](https://doi.org/10.1016/S0377-0273(99)00037-2)
- Di Vito MA, Arienzo I, Braia G, Civetta L, D'Antonio M, Di Renzo V, Orsi G (2011) The Averno 2 fissure eruption: a recent small-size explosive event at the Campi Flegrei caldera (Italy). *Bull Volcanol* 73:295–320. <https://doi.org/10.1007/s00445-010-0417-0>
- Di Vito M, Acocella V, Aiello G, Barra D, Battaglia M, Carandente A, Del Gaudio C, de Vita S, Ricciardi GP, Ricco C, Scandone R, Terrasi F (2016) Magma transfer at Campi Flegrei caldera (Italy) before the 1538 AD eruption. *Sci Rep* 6:32245. <https://doi.org/10.1038/srep32245>
- Esposti Ongaro T, Papale P, Neri A, Del Seppia D (2006) Influence of carbon dioxide on the large-scale dynamics of magmatic eruptions at Phlegrean Fields (Italy). *Geophys Res Lett* 33:L06318. <https://doi.org/10.1029/2005GL025528>
- Esposti Ongaro T, Cavazzoni C, Erbacci G, Neri A, Salvetti MV (2007) A parallel multiphase flow code for the 3D simulation of volcanic explosive eruptions. *Parallel Comput* 33(7–8):541–560. <https://doi.org/10.1016/j.parco.2007.04.003>
- Esposti Ongaro T, Neri A, Menconi G, de' Michieli Vitturi M, Marianelli P, Cavazzoni C, Erbacci G, Baxter PJ (2008) Transient 3D numerical simulations of column collapse and pyroclastic density current scenarios at Vesuvius. *J Volcanol Geotherm Res* 178(3):378–396. <https://doi.org/10.1016/j.jvolgeores.2008.06.036>
- Esposti Ongaro T, Orsucci S, Cornolti F (2016) A fast, calibrated model for pyroclastic density currents kinematics and hazard. *J Volcanol Geotherm Res* 327:257–272. <https://doi.org/10.1016/j.jvolgeores.2016.08.002>
- Esposti Ongaro T, Komorowski JC, Legendre Y, Neri A (2020) Modelling pyroclastic density currents from a subplinian eruption at La Soufrière de Guadeloupe (West Indies, France). *Bull Volcanol* 82:76. <https://doi.org/10.1007/s00445-020-01411-6>
- Fedele L, Scarpati C, Lanphere M, Melluso L, Morra V, Perrotta A, Ricci G (2008) The Breccia Museo formation, Campi Flegrei, Southern Italy: geochronology, chemostratigraphy and relationship with the Campanian Ignimbrite eruption. *Bull Volcanol* 70:1189–1219. <https://doi.org/10.1007/s00445-008-0197-y>
- Fedele L, Insinga DD, Calvert AT, Morra V, Perrotta A, Scarpati C (2011) $^{40}\text{Ar}/^{39}\text{Ar}$ dating of tuff vents in the Campi Flegrei caldera (Southern Italy): toward a new chronostratigraphic reconstruction of the Holocene volcanic activity. *Bull Volcanol* 73:1323–1336. <https://doi.org/10.1007/s00445-011-0478-8>
- Fedele L, Insinga DD, Calvert AT, Morra V, Perrotta A, Scarpati C (2012) Reply to the comment on the article “ $^{40}\text{Ar}/^{39}\text{Ar}$ dating of tuff vents in the Campi Flegrei caldera (southern Italy): toward a new chronostratigraphic reconstruction of the Holocene volcanic activity” by Isaia et al. *Bull Volcanol* 74:297–299. <https://doi.org/10.1007/s00445-011-0560-2>
- Fisher RV, Orsi G, Ort M, Heiken G (1993) Mobility of large-volume pyroclastic flow—emplacement of the Campanian Ignimbrite, Italy. *J Volcanol Geotherm Res* 56:205–220. [https://doi.org/10.1016/0377-0273\(93\)90017-L](https://doi.org/10.1016/0377-0273(93)90017-L)
- Flueck WY (2016) Brief communication: extended chronology of the Cordón Caulle volcanic eruption beyond 2011 reveals toxic impacts. *Nat Haz Earth Sys Sci* 16:2351–2355. <https://doi.org/10.5194/nhess-16-2351-2016>
- Folch A, Costa A, Macedonio G (2009) FALL3D: A computational model for transport and deposition of volcanic ash. *Comput Geosci* 35:1334–1342. <https://doi.org/10.1016/j.cageo.2008.08.008>
- Folch A, Sulpizio R (2010) Evaluating the long-range volcanic ash hazard using supercomputing facilities. Application to Somma-Vesuvius (Italy), and consequences on civil aviation over the Central Mediterranean Area. *Bull Volcanol* 72:1039–1059. <https://doi.org/10.1007/s00445-010-0386-3>
- Fournier d'Albe EM (1979) Objectives of volcano monitoring and prediction. *J Geol Soc London* 136:321–326. <https://doi.org/10.1144/gsjgs.136.3.0321>
- Geyer A, Marti J (2008) The new worldwide collapse caldera database (CCDB): A tool for studying and understanding caldera processes. *J Volcanol Geotherm Res* 175(3):334–354. <https://doi.org/10.1016/j.jvolgeores.2008.03.017>
- Giaccio B, Hajdas I, Isaia R, Deino A, Nomade S (2017) High-precision ^{14}C dating and $^{40}\text{Ar}/^{39}\text{Ar}$ dating of the Campanian Ignimbrite (Y-5) reconciles the time-scales of climatic-cultural processes at 40 ka. *Sci Rep* 7:45940. <https://doi.org/10.1038/srep45940>
- Giudicepietro F, Macedonio G, D'Auria L, Martini M (2016) Insight into vent opening probability in volcanic calderas in the light of a sill intrusion model. *Pure Appl Geophys* 173:1703–1720. <https://doi.org/10.1007/s00024-015-1190-y>
- Giudicepietro F, Macedonio G, Martini M (2017) A physical model of sill expansion to explain the dynamics of unrest at calderas with application to Campi flegrei. *Front Earth Sc-Switz* 5:54–65. <https://doi.org/10.3389/feart.2017.00054>
- Giudicepietro F, Chiodini G, Caliro S, De Cesare W, Esposito AM, Galluzzo D, Lo Bascio D, Macedonio G,

- Orazi M, Ricciolino P, Vandemeulebrouck J (2019) Insight into Campi Flegrei Caldera Unrest through seismic tremor measurements at Pisciarelli Fumarolic Field. *Geochem Geophys Geosys* 20:5544–5555. <https://doi.org/10.1029/2019GC008610>
- Giudicepietro F, Chiodini G, Avino R, Brandi G, Caliro S, De Cesare W, Galluzzo D, Esposito A, La Rocca A, Lo Bascio D, Obrizzo F, Pinto S, Ricci T, Ricciolino P, Siniscalchi A, Tramelli A, Vandemeulebrouck J, Macedonio G (2021) Tracking episodes of seismicity and gas transport in Campi Flegrei caldera through seismic, geophysical, and geochemical measurements. *Seismol Res Lett* 92(2A):965–975. <https://doi.org/10.1785/0220200223>
- Guidoboni E, Ciuccarelli C (2011) The Campi Flegrei caldera: historical revision and new data on seismic crises, bradyseisms, the Monte Nuovo eruption and ensuing earthquakes (twelfth century 1582 AD). *Bull Volcanol* 73:655–677. <https://doi.org/10.1007/s00445-010-0430-3>
- Heiken G, Fakundiny R, Sutter J (eds.) (2003) *Earth Sciences in the Cities: A Reader*. Am Geophys Un, Sp Publ Series 56, 444 pp. <https://doi.org/10.1029/SP056>
- Houghton B, White JDL, Van Eaton AR (2015) Phreatomagmatic and related eruption styles. In: Sigurdsson H, Houghton B, McNutt S, Rymer H, Stix J (eds) *Encyclopaedia of Volcanoes*, 2nd ed. Academic Press, San Diego (CA), USA, pp 537–552. <https://doi.org/10.1016/B978-0-12-385938-9.00030-4>
- Huppert HE, Simpson JE (1980) The slumping of gravity currents. *J Fluid Mech* 99(4):785–799
- Kilburn CRJ (2018) Forecasting volcanic eruptions: beyond the failure forecast method. *Front Earth Sc-Switz* 6:133. <https://doi.org/10.3389/feart.2018.00133>
- Kilburn C, De Natale G, Carlino S (2017) Progressive approach to eruption at Campi Flegrei caldera in southern Italy. *Nat Commun* 8:15312. <https://doi.org/10.1038/ncomms15312>
- Granieri D, Costa A, Macedonio G, Bisson M, Chiodini G (2013) Carbon dioxide in the urban area of Naples: Contribution and effects of the volcanic source. *J Volcanol Geotherm Res* 260:52–61. <https://doi.org/10.1016/j.jvolgeores.2013.05.003>
- Isaia R, D'Antonio M, Dell'Erba F, Di Vito MA, Orsi G (2004) The Astroni volcano: the only example of close eruptions within the same vent area in the recent history of the Campi Flegrei caldera (Italy). *J Volcanol Geotherm Res* 133:171–192. [https://doi.org/10.1016/S0377-0273\(03\)00397-4](https://doi.org/10.1016/S0377-0273(03)00397-4)
- Isaia R, Marianelli P, Sbrana A (2009) Caldera unrest prior to intense volcanism in Campi Flegrei (Italy) at 4.0 ka B.P.: Implications for caldera dynamics and future eruptive scenarios. *Geophys Res Lett* 36: L21303. <https://doi.org/10.1029/2009GL040513>
- Isaia R, Di Vito MA, de Vita S, Rosi M, Sbrana A (2012) Comment on “ $^{40}\text{Ar}/^{39}\text{Ar}$ dating of tuff vents in the Campi Flegrei caldera (southern Italy): Toward a new chronostratigraphic reconstruction of the Holocene volcanic activity” by Fedele et al. [*Bull Volcanol* 73:1323–1336]. *Bull Volcanol* 74:293–296. <https://doi.org/10.1007/s00445-011-0561-1>
- Isaia R, Vitale S, Di Giuseppe MG, Iannuzzi E, Tramparulo F, Troiano A (2015) Stratigraphy, structure, and volcano-tectonic evolution of Solfatara maar-diatreme (Campi Flegrei, Italy). *Geol Soc Am Bull* 127:1485–1504. <https://doi.org/10.1130/B31183.1>
- Isaia R, Vitale S, Marturano A, Aiello G, Barra D, Ciarcia S, Iannuzzi E, D'Assisi Tramparulo F (2019) High-resolution geological investigations to reconstruct the long-term ground movements in the last 15 kyr at Campi Flegrei caldera (southern Italy). *J Volcanol Geotherm Res* 385:143–158. <https://doi.org/10.1016/j.jvolgeores.2019.07.012>
- ISDR 2005 Hyogo Framework for Action 2005–2015: ISDR international strategy for disaster reduction: building the resilience of nations and communities to disasters. <https://www.unisdr.org/2005/wcdtr/intergover/official-doc/L-docs/Hyogo-framework-for-action-english.pdf>. Last accessed February 8th 2020
- Jolly G, De La Cruz S (2015) Volcanic crisis management. In: Sigurdsson H, Houghton B, McNutt S, Rymer H, Stix J (eds) *Encyclopaedia of Volcanoes*, 2nd ed. Academic Press, San Diego (CA), USA, pp 1188–1202. <https://doi.org/10.1016/B978-0-12-385938-9.00068-7>
- Le Guern F, Tazieff H, Fivre-Pierret R (1982) An example of health hazard: people killed by gas during a phreatic eruption: Dieng Plateau (Java, Indonesia), Feb. 20 1979. *Bull Volcanol* 45:153–156. <https://doi.org/10.1007/BF02600430>
- Lirer L, Petrosino P, Alberico I (2001) Hazard assessment at volcanic fields: the Campi Flegrei case history. *J Volcanol Geotherm Res* 112:53–74. [https://doi.org/10.1016/S0377-0273\(01\)00234-7](https://doi.org/10.1016/S0377-0273(01)00234-7)
- Lirer L, Petrosino P, Alberico I (2010) Hazard and risk assessment in a complex multi-source volcanic area: the example of the Campania Region, Italy. *Bull Volcanol* 72:411–429. <https://doi.org/10.1007/s00445-009-0334-2>
- Macedonio G, Costa A (2012) Brief Communication: Rain effect on the load of tephra deposits. *Nat Haz Earth Sys Sci* 12:1229–1233. <https://doi.org/10.5194/nhess-12-1229-2012>
- Macedonio G, Costa A, Longo A (2005) A computer model for volcanic ash fallout and assessment of subsequent hazard. *Comput Geosci* 31:837–845. <https://doi.org/10.1016/j.cageo.2005.01.013>
- Macedonio G, Martini M, Neri A, Papale P, Rosi M, Zuccaro G (2013) Rapporto Finale. Gruppo di Lavoro incaricato della definizione dello scenario di riferimento per il piano di emergenza dei Campi Flegrei per il rischio vulcanico. 122 pp. http://www.protezionecivile.gov.it/resources/cms/documents/rapporto_GdL_CampiFlegrei_art_70_def.pdf
- Macedonio G, Giudicepietro F, D'Auria L, Martini M (2014) Sill intrusion as a source mechanism of unrest at volcanic calderas. *J Geophys Res Solid Earth* 119:3986–4000. <https://doi.org/10.1002/2013JB010868>

- Macedonio G, Costa A, Scollo S, Neri A (2016) Effects of eruption source parameter variation and meteorological dataset on tephra fallout hazard assessment: an example from Vesuvius, Italy. *J Appl Volcanol* 5:1–19. <https://doi.org/10.1186/s13617-016-0045-2>
- Mayer K, Scheu B, Montanaro C, Yilmaz T, Isaia R, Aßbichler D, Dingwell DB (2016) Hydrothermal alteration of surficial rocks at Solfatara (Campi Flegrei): Petrophysical properties and implications for phreatic eruption processes. *J Volcanol Geotherm Res* 320:128–143. <https://doi.org/10.1016/j.jvolgeores.2016.04.020>
- Mastrolorenzo G, Pappalardo L, Troise C, Rossano S, Panizza A, De Natale G (2006) Volcanic hazard assessment at the Campi Flegrei caldera. In Troise C, De Natale G, Kilburn CRJ (eds). *Mechanisms of Activity and Unrest at Large Calderas*. *Geol Soc Lond Spec Publ* 269:159–171. <https://doi.org/10.1144/GSL.SP.2006.269.01.10>
- Mastrolorenzo G, Pappalardo L, Troise C, Panizza A, De Natale G (2008) Probabilistic tephra hazard maps for the Neapolitan area: Quantitative volcanological study of Campi Flegrei eruptions. *J Geophys Res* 113: B07203. <https://doi.org/10.1029/2007JB004954>
- Mastrolorenzo G, Palladino DM, Pappalardo L, Rossano S (2017) Probabilistic-numerical assessment of pyroclastic current hazard at Campi Flegrei and Naples city: Multi-VEI scenarios as a tool for “full-scale” risk management. *PLoS ONE* 12(10):e0185756. <https://doi.org/10.1371/journal.pone.0185756>
- Marti J, Ernst GGJ (2005) *Volcanoes and the environment*. Cambridge University Press, Cambridge, UK, pp 1–471
- Marzocchi W, Bebbington MS (2012) Probabilistic eruption forecasting at short and long time scales. *Bull Volcanol* 74:1777–1805. <https://doi.org/10.1007/s00445-012-0633-x>
- Marzocchi W, Sandri L, Selva J (2010) BET_VH: a probabilistic tool for long-term volcanic hazard assessment. *Bull Volcanol* 72:705–716. <https://doi.org/10.1007/s00445-010-0357-8>
- Marzocchi W, Taroni M, Selva J (2015a) Accounting for epistemic uncertainty in PSHA. Logic tree and ensemble modeling. *B Seismol Soc Am* 104:2151–2159. <https://doi.org/10.1785/0120140131>
- Marzocchi W, Selva J, Costa A, Sandri L, Tonini R, Macedonio G (2015b) Tephra fall hazard for the Neapolitan area. In: Loughlin SC, Sparks RSJ, Brown SK, Jenkins SF, Vye-Brown C (eds) *Global volcanic hazards and risk*, Cambridge University Press, Cambridge, UK, pp 239–247. <https://doi.org/10.1017/CBO9781316276273.008>
- McGuire WJ, Kilburn CRJ, Murray JB (1995) Monitoring active volcanoes: strategies, procedures and techniques. *Univ College London Press*, London, UK, 420 pp. [https://doi.org/10.1002/\(SICI\)1096-9837\(199609\)21:9<874::AID-ESP583>3.0.CO;2-I](https://doi.org/10.1002/(SICI)1096-9837(199609)21:9<874::AID-ESP583>3.0.CO;2-I)
- Mele D, Dioguardi F, Dellino P, Isaia R, Sulpizio R, Braia G (2015) Hazard of pyroclastic density currents at the Campi Flegrei caldera (southern Italy) as deduced from the combined use of face architecture, physical modeling and statistics of the impact parameters. *J Volcanol Geotherm Res* 299:35–53. <https://doi.org/10.1016/j.jvolgeores.2015.04.002>
- Montanaro C, Scheu B, Mayer K, Orsi G, Moretti R, Isaia R, Dingwell DB (2016) Experimental investigations on the explosivity of steam-driven eruptions: A case study of Solfatara volcano (Campi Flegrei). *J Geophys Res Solid Earth* 121:7996–8014. <https://doi.org/10.1002/2016JB013273>
- Nairn IA, McKee CO, Talai B, Wood CP (1995) Geology and eruptive history of the 550 Rabaul Caldera area, Papua New Guinea. *J Volcanol Geotherm Res* 69:255–284. [https://doi.org/10.1016/0377-0273\(95\)00035-6](https://doi.org/10.1016/0377-0273(95)00035-6)
- Natale J, Ferranti L, Marino C, Sacchi M (2020) Resurgent-dome faults in the offshore of the Campi Flegrei caldera (Pozzuoli Bay, Campania): preliminary results from high-resolution seismic reflection profiles. *Boll Geof Teor Appl* 61(3):333–342. <https://doi.org/10.4430/bgta0315>
- National Academies of Sciences, Engineering, and Medicine (2017) *Volcanic eruptions and their repose, unrest, precursors, and timing*. The National Academies Press, Washington, DC, USA, pp 1–122. <https://doi.org/10.17226/24650>
- Neri A, Macedonio G, Gidaspow D (1999) Phreatic explosions hazard assessment by numerical simulation. *Phys Chem Earth* 24(11–12):989–995. [https://doi.org/10.1016/S1464-1895\(99\)00147-7](https://doi.org/10.1016/S1464-1895(99)00147-7)
- Neri A, Esposti Ongaro T, Menconi G, de’ Michieli Vitturi M, Cavazzoni C, Erbacci G, Baxter PJ (2007) 4D Simulation of explosive eruption dynamics at Vesuvius. *Geophys Res Lett* 34. <https://doi.org/10.1029/2006GL028597>
- Neri A, Esposti Ongaro T, Voight B, Widiwijayanti C (2015a) Pyroclastic density current hazards and risk. In: Papale P, Schroder J (eds) *Volcanic hazards, risks and disasters*. Elsevier, London, UK, 5:109–140. <https://doi.org/10.1016/B978-0-12-396453-3.00005-8>
- Neri A, Bevilacqua A, Esposti Ongaro T, Isaia R, Aspinall WP, Bisson M, Flandoli F, Baxter PJ, Bertagnini A, Iannuzzi E, Orsucci S, Pistolesi M, Rosi M, Vitale S (2015b) Quantifying volcanic hazard at Campi Flegrei caldera (Italy) with uncertainty assessment: 2. Pyroclastic density current invasion maps. *J Geophys Res* 120:2330–2349. <https://doi.org/10.1002/2014JB011776>
- Neri A, Esposti Ongaro T, de’ Michieli Vitturi M, Cerminara M. (2021) Multiphase flow modeling of explosive volcanic eruptions, In: Arastoopour H, Gidaspow D, Lyczkowski (eds) *Transport phenomena in multiphase systems*. Mechanical Engineering Series, Springer. ISBN 978–3–030–68578–2
- Newhall CG, Dzurisin D (1988a) *Historical Unrest at Large Calderas of the World*, volume 1. USGS Bulletin, Washington, (DC). USA 1855:1–610
- Newhall CG, Dzurisin D (1988b) *Historical unrest at large calderas of the world*, volume 2. USGS Bulletin, Washington, (DC). USA 1855:1–520

- Orsi G, D'Antonio M, de Vita S, Gallo G (1992) The Neapolitan Yellow Tuff, a large-magnitude trachytic phreatoplinian eruption: eruptive dynamics, magma withdrawal and caldera collapse. *J Volcanol Geotherm Res* 53:275–287. [https://doi.org/10.1016/0377-0273\(92\)90086-S](https://doi.org/10.1016/0377-0273(92)90086-S)
- Orsi G, Civetta L, D'Antonio M, Di Girolamo P, Piochi M (1995) Step-filling and development of a three-layers magma chamber: the Neapolitan Yellow Tuff case history. *J Volcanol Geotherm Res* 67:291–312. [https://doi.org/10.1016/0377-0273\(94\)00119-2](https://doi.org/10.1016/0377-0273(94)00119-2)
- Orsi G, de Vita S, Di Vito M (1996) The restless, resurgent Campi Flegrei nested caldera (Italy): constraints on its evolution and configuration. *J Volcanol Geotherm Res* 74:179–214. [https://doi.org/10.1016/S0377-0273\(96\)00063-7](https://doi.org/10.1016/S0377-0273(96)00063-7)
- Orsi G, Civetta L, Del Gaudio C, de Vita S, Di Vito MA, Isaia R, Petrazzuoli SM, Ricciardi G, Ricco C (1999) Short-term ground deformations and seismicity in the nested Campi Flegrei caldera (Italy): an example of active block-resurgence in a densely populate area. *J Volcanol Geotherm Res* 91:415–451. [https://doi.org/10.1016/S0377-0273\(99\)00050-5](https://doi.org/10.1016/S0377-0273(99)00050-5)
- Orsi G, de Vita S, Di Vito M, Isaia R, Nave R, Heiken G (2003) Facing volcanic and related hazards in the Neapolitan area. In: Heiken G, Fakundiny R, Sutter J (eds) *Earth sciences in the cities: a reader*. Am Geophys Un, Sp Publ Series, 56:121–170, ISBN 0–87590–299–5
- Orsi G, Di Vito MA, Isaia R (2004) Volcanic hazard assessment at the restless Campi Flegrei caldera. *Bull Volcanol* 66:514–530. <https://doi.org/10.1007/s00445-003-0336-4>
- Orsi G, Di Vito MA, Selva J, Marzocchi W (2009) Long-term forecast of eruption style and size at Campi Flegrei caldera (Italy). *Earth Planet Sci Lett* 287:265–276. <https://doi.org/10.1016/j.epsl.2009.08.013>
- Pallister J, McNutt SR (2015) Synthesis of Volcano Monitoring. In: Sigurdsson H, Houghton B, McNutt SR, Rymer H, Stix J (eds) *Encyclopedia of Volcanoes*, 2nd ed. Academic Press, San Diego (CA), USA, pp 1151–1171. <https://doi.org/10.1016/B978-0-12-385938-9.00066-3>
- Paris R, Ulvrova M, Selva J, Brizuela B, Costa A, Grezio A, Lorito S, Tonini R (2019) Probabilistic hazard analysis for tsunamis generated by subaqueous volcanic explosions in the Campi Flegrei caldera, Italy. *J Volcanol Geotherm Res* 379:106–116. <https://doi.org/10.1016/j.jvolgeores.2019.05.010>
- Patra A, Bevilacqua A, Pitman EB, Bursik B, Voight B, Neri A, Macedonio G, Flandoli F, De Martino P, Giudicepietro F, Vitale S (2019) A statistical approach for spatial mapping and temporal forecasts of volcanic eruptions using monitoring data. AGU 2019 Fall Meeting, San Francisco, CA, USA, 9–13 December 2019. <https://doi.org/10.1002/essoar.10502434.1>
- Perrotta A, Scarpato C, Luongo G, Morra V (2010) Stratigraphy and volcanological evolution of the southern sector of Campi Flegrei and Procida Island, Italy. In: Groppelli G, Viereck-Goette L (eds) *Stratigraphy and geology of volcanic areas*. Geol Soc Am Sp Paper 464:171–191. [https://doi.org/10.1130/2010.2464\(09\)](https://doi.org/10.1130/2010.2464(09))
- Perugini D, Petrelli M, Poli G, De Campos CP, Dingwell DB (2010) Time-scales of recent Phlegrean Fields eruptions inferred by the application of the 'diffusive fractionation' model of trace elements. *Bull Volcanol* 72:431–447. <https://doi.org/10.1007/s00445-009-0329-z>
- Pistolesi M, Isaia R, Marianelli P, Bertagnini A, Fourmentraux C, Albert P, Tomlinson E, Menzies M, Rosi M, Sbrana A (2016) Simultaneous eruptions from multiple vents at Campi Flegrei (Italy) highlight new eruption processes at calderas. *Geology* 44(6):487–490. <https://doi.org/10.1130/G37870.1>
- Pistolesi M, Bertagnini A, Di Roberto A, Vona A, Cioni R, Giordano G (2017) The Baia-Fondi di Baia eruption at Campi Flegrei: stratigraphy and dynamics of a multi-stage caldera reactivation event. *Bull Volcanol* 79:67. <https://doi.org/10.1007/s00445-017-1149-1>
- Poland M, Anderson K (2020) Partly cloudy with a chance of lava flows: Forecasting volcanic eruptions in the twenty-first century. *J Geophys Res Solid Earth* 125(1):e2018JB016974. <https://doi.org/10.1029/2018JB016974>
- Queißer M, Granieri D, Burton M, Arzilli F, Avino R, Carandente A (2017) Increasing CO₂ flux at Pisciarelli, Campi Flegrei, Italy. *Solid Earth* 8:1017–1024. <https://doi.org/10.5194/se-8-1017-2017>
- Ricco C, Petrosino S, Aquino I, Del Gaudio C, Falanga F (2019) Some investigations on a possible relationship between ground deformation and seismic activity at Campi Flegrei and Ischia volcanic areas (Southern Italy). *Geosciences* 9(5):222. <https://doi.org/10.3390/geosciences9050222>
- Rivalta E, Corbi F, Passarelli L, Acocella V, Davis T, Di Vito MA (2019) Stress inversions to forecast magma pathways and eruptive vent location. *Sci Adv* 5:7. <https://doi.org/10.1126/sciadv.aau97>
- Robertson RM, Kilburn CR (2016) Deformation regime and long-term precursors to eruption at large calderas: Rabaul, Papua New Guinea. *Earth Planet Sci Lett* 438:86–94. <https://doi.org/10.1016/j.epsl.2016.01.003>
- Romano C, Vona A, Campagnola S, Giordano G, Arienzo I, Isaia R (2020) Modelling and physico-chemical constraints to the 4.5 ka Agnano-Monte Spina Plinian eruption (Campi Flegrei, Italy). *Chem Geol* 532:119301. <https://doi.org/10.1016/j.chemgeo.2019.119301>
- Rosi M, Santacroce R (1984) Volcanic hazard assessment in the Phlegraean Fields: a contribution based on stratigraphic and historical data. *Bull Volcanol* 47:359–370. <https://doi.org/10.1007/BF01961567>
- Rosi M, Sbrana A (eds) (1987) *Phlegrean Fields*. Quaderni de "La Ricerca Scientifica" CNR, Rome, Italy, 114:1–175. ISSN 0556–9664

- Rosi M, Vezzoli L, Aleotti P, De Censi M (1996) Interaction between caldera collapse and eruptive dynamics during the Campanian Ignimbrite eruption, Phlegraean Fields, Italy. *Bull Volcanol* 57:541–554. <https://doi.org/10.1007/BF00304438>
- Rossano S, Mastrolorenzo G, De Natale G (2004) Numerical simulation of pyroclastic density currents on Campi Flegrei topography: A tool for statistical hazard estimation. *J Volcanol Geotherm Res* 132:1–14. [https://doi.org/10.1016/S0377-0273\(03\)00384-6](https://doi.org/10.1016/S0377-0273(03)00384-6)
- Rutherford MJ (2004) Experimental petrology studies. In: Papale, P. *Rapporto finale del progetto GNV 2001–03 n. 17 “Simulation of Eruptive Scenarios at Phlegraean Fields Based on Field, Laboratory, and Numerical Studies, and Implications for Volcanic Hazard”*
- Sacchi M, Pepe F, Corradino M, Insinga DD, Molisso F, Lubritto C (2014) The Neapolitan Yellow Tuff caldera offshore the Campi Flegrei: Stratal architecture and kinematic reconstruction during the last 15 ky. *Mar Geol* 354:15–33. <https://doi.org/10.1016/j.margeo.2014.04.012>
- Sandri L, Costa A, Selva J, Tonini R, Macedonio G, Folch A, Sulpizio R (2016) Beyond eruptive scenarios: assessing tephra fallout hazard from Neapolitan Volcanoes. *Sci Rep* 6:24271. <https://doi.org/10.1038/srep24271>
- Sandri L, Tierz P, Costa A, Marzocchi W (2018) Probabilistic hazard from pyroclastic density currents in the Neapolitan area (Southern Italy). *J Geophys Res Solid Earth* 123:3474–3500. <https://doi.org/10.1002/2017JB014890>
- Sandri L, Bevilacqua A, Selva J, Neri A, Costa A, Macedonio G (2020) Eruption forecasting and hazard assessment at INGV during the 2019 crisis exercise at Campi Flegrei. 4th Rittmann Conference, Miscelanea INGV 52, ISSN 2039–6651, Catania, Italy, 12–14 February 2020, <http://hdl.handle.net/2122/13862>
- Scandone R, D’Amato J, Giacomelli L (2010) The relevance of the 1198 eruption of Solfatara in the Phlegraean Fields (Campi Flegrei) as revealed by medieval manuscripts and historical sources. *J Volcanol Geotherm Res* 189(1–2):202–206. <https://doi.org/10.1016/j.jvolgeoes.2009.09.012>
- Scarpa R, Tilling RI (eds.) (1996) *Monitoring and mitigation of volcano hazards*. Springer-Verlag, Heidelberg, Germany, 841 pp, ISBN 978–3–642–80087–0
- Scarpato C, Cole P, Perrotta A (1993) The Neapolitan Yellow Tuff - A large volume multiphase eruption from Campi Flegrei, Southern Italy. *Bull Volcanol* 55:343–356. <https://doi.org/10.1007/BF00301145>
- Selva J, Costa A, Marzocchi W, Sandri L (2010) BET_VH: Exploring the influence of natural hazard uncertainties on long-term hazard from tephra fallout at Campi Flegrei, (Italy). *Bull Volcanol* 72:717–733. <https://doi.org/10.1007/s00445-010-0358-7>
- Selva J, Marzocchi W, Papale P, Sandri L (2012a) Operational eruption forecasting at high-risk volcanoes: the case of Campi Flegrei. Naples. *J Appl Volcanol* 1:5. <https://doi.org/10.1186/2191-5040-1-5>
- Selva J, Orsi G, Di Vito M, Marzocchi W, Sandri L (2012b) Probability hazard map for future vent opening at the Campi Flegrei caldera. Italy. *Bull Volcanol* 74(2):497–510. <https://doi.org/10.1007/s00445-011-0528-2>
- Selva J, Marzocchi W, Sandri L, Costa A (2015) Operational short-term volcanic hazard analysis: methods and perspectives. In: Shroder JF, Papale P (eds) *Volcanic Hazards, Risks and Disasters*, Ch. 9. Elsevier, New York, USA, pp 233–259. <https://doi.org/10.1016/B978-0-12-396453-3.00009-5>
- Selva J, Costa A, De Natale G, Di Vito MA, Isaia R, Macedonio G (2018) Sensitivity test and ensemble hazard assessment for tephra fallout at Campi Flegrei, Italy. *J Volcanol Geotherm Res* 351:1–28. <https://doi.org/10.1016/j.jvolgeoes.2017.11.024>
- Sheridan MF, Malin MC (1983) Application of computer-assisted mapping to volcanic hazard evaluation of surge eruptions: Vulcano, Lipari, and Vesuvius. *J Volcanol Geotherm Res* 17(1):187–202. [https://doi.org/10.1016/0377-0273\(83\)90067-7](https://doi.org/10.1016/0377-0273(83)90067-7)
- Siebert L, Simkin T, Kimberly P (2010) *Volcanoes of the World*, 3rd edn. Smithsonian Institution, Berkeley, CA, USA
- Siebert L, Cottrell E, Venzke E, Andrews B (2015) Earth’s Volcanoes and Their Eruptions: An Overview. In: Sigurdsson H, Houghton B, McNutt S, Rymer H, Stix J (eds) *Encyclopaedia of Volcanoes*, 2nd ed. Academic Press, San Diego, CA, USA, pp. 239–255. <https://doi.org/10.1016/B978-0-12-385938-9.00012-2>
- Silleni A, Giordano G, Isaia R, Ort MH (2020) The Magnitude of the 39.8 ka Campanian Ignimbrite Eruption, Italy: Method, Uncertainties and Errors. *Front Earth Sc-Switz* 8:543399. <https://doi.org/10.3389/feart.2020.543399>
- Simkin T, Siebert L (1994) *Volcanoes of the World: A Regional Directory, Gazetteer, and Chronology of Volcanism During the Last 10,000 Years* (Second Edition). Smithsonian Inst Geosci Press Inc., Tucson, AZ, USA, p 349
- Small C, Naumann T (2001) The global distribution of human population and recent volcanism. *Global Environ Chang Part b, Environ Haz* 3:93–109. [https://doi.org/10.1016/S1464-2867\(02\)00002-5](https://doi.org/10.1016/S1464-2867(02)00002-5)
- Smith VC, Isaia R, Pearce NJG (2011) Tephrostratigraphy and glass compositions of post-15 kyr Campi Flegrei eruptions: implications for eruption history and chronostratigraphic markers. *Quaternary Sci Rev* 30:3638–3660. <https://doi.org/10.1016/j.quascirev.2011.07.012>
- Sparks RSJ (2003) Forecasting volcanic eruptions. *Earth Planet Sci Lett* 210:1–15. [https://doi.org/10.1016/S0012-821X\(03\)00124-9](https://doi.org/10.1016/S0012-821X(03)00124-9)
- Sparks RSJ, Biggs J, Neuberg JW (2012) Monitoring Volcanoes. *Science* 335(6074):1310–1311. <https://doi.org/10.1126/science.1219485>
- Spence RJS, Kelman I, Baxter PJ, Zuccaro G, Petrazzuoli S (2005) Residential building and occupant vulnerability to tephra fall. *Nat Haz Earth Sys Sc* 5:477–494. <https://doi.org/10.5194/nhess-5-477-2005>

- Steinmann L, Spiess V, Sacchi M (2018) Post-collapse evolution of a coastal caldera system: Insights from a 3D multichannel seismic survey from the Campi Flegrei caldera (Italy). *J Volcanol Geotherm Res* 349:83–98. <https://doi.org/10.1016/j.jvolgeores.2017.09.023>
- Sulpizio R, Dellino P, Doronzo DM, Sarocchi D (2014) Pyroclastic density currents: state of the art and perspectives. *J Volcanol Geotherm Res* 283:36–65. <https://doi.org/10.1016/j.jvolgeores.2014.06.014>
- Tadini A, Bevilacqua A, Neri A, Cioni R, Biagioli G, de' Michieli Vitturi M, Esposti Ongaro T (2021) Reproducing pyroclastic density currents deposits of the AD 79 eruption of the Somma-Vesuvius volcano using the box-model approach. *Solid Earth* 12:119–139. <https://doi.org/10.5194/se-12-119-2021>
- Tamburello G, Caliro S, Chiodini G, De Martino P, Avino R, Minopoli C, Carandente A, Rouwet D, Aiuppa A, Costa A, Bitetto M, Giudice G, Francofonte V, Ricci T, Sciarra A, Bagnato E, Capecchiacci F (2019) Escalating CO₂ degassing at the Pisciarelli fumarolic system, and implications for the ongoing Campi Flegrei unrest. *J Volcanol Geotherm Res* 384:151–157. <https://doi.org/10.1016/j.jvolgeores.2019.07.005>
- Tierz P, Sandri L, Costa A, Zaccarelli L, Di Vito MA, Sulpizio R, Marzocchi W (2016) Suitability of energy cone for probabilistic volcanic hazard assessment: validation tests at Somma-Vesuvius and Campi Flegrei (Italy). *Bull Volcanol* 78:79. <https://doi.org/10.1007/s00445-016-1073-9>
- Tilling RI (2001) *Volcano monitoring and eruption warnings*. Springer-Verlag, Berlin Heidelberg, Germany, pp 505–510. <https://doi.org/10.1007/978-3-642-55903-766>
- Todesco M, Neri A, Esposti Ongaro T, Papale P, Rosi M (2006) Pyroclastic flow dynamics and hazard in a caldera setting: application to Phlegrean Fields (Italy). *Geochem Geophys Geosys* 7:11. <https://doi.org/10.1029/2006GC001314>
- Tonarini S, D'Antonio M, Di Vito MA, Orsi G, Carandente A (2009) Geochemical and isotopic (B, Sr, Nd) evidence for mixing and mingling processes in the magmatic system feeding the Astroni volcano (4.1–3.8 ka) within the Campi Flegrei caldera (South Italy). *Lithos* 107:135–151. <https://doi.org/10.1016/j.lithos.2008.09.012>
- Tonini R, Sandri L, Costa A, Selva J (2015) Brief Communication: The effect of submerged vents on probabilistic hazard assessment for tephra fallout. *Nat Hazards Earth Syst Sci* 15:409–415. <https://doi.org/10.5194/nhess-15-409-2015>
- Vitale S, Isaia R (2014) Fractures and faults in volcanic rocks (Campi Flegrei, Southern Italy): Insights into volcano-tectonic processes. *Int J Earth Sci* 103:801–819. <https://doi.org/10.1007/s00531-013-0979-0>
- Vitale S, Isaia R, Ciarcia S, Di Giuseppe MG, Iannuzzi E, Prinzi EP, Tramparulo FDA, Troiano A (2019) Seismically induced soft-sediment deformation phenomena during the volcano-tectonic activity of Campi Flegrei caldera (southern Italy) in the last 15 kyr. *Tectonics* 38:1999–2018. <https://doi.org/10.1029/2018TC005267>
- Voight B (1988) A method for prediction of volcanic eruptions. *Nature* 332:125–130. <https://doi.org/10.1038/332125a0>
- Voloschina M, Pistolesi M, Bertagnini A, Métrich N, Pompilio M, Di Roberto A, Di Salvo S, Francalanci L, Isaia R, Cioni R, Romano C (2018) Magmatic reactivation of the Campi Flegrei volcanic system: insights from the Baia-Fondi di Baia eruption. *Bull Volcanol* 80:75. <https://doi.org/10.1007/s00445-018-1247-8>
- Wohletz K, Orsi G, de Vita S (1995) Eruptive mechanisms of the Neapolitan Yellow Tuff interpreted from stratigraphic, chemical and granulometric data. *J Volcanol Geotherm Res* 67:263–290. [https://doi.org/10.1016/0377-0273\(95\)00002-C](https://doi.org/10.1016/0377-0273(95)00002-C)
- Williams-Jones G, Rymer H (2015) Hazards of Volcanic Gases. In: Sigurdsson H, Houghton B, McNutt S, Rymer H, Stix J (eds) *Encyclopaedia of Volcanoes*, 2nd ed. Academic Press, San Diego, CA, USA, pp 985–992. <https://doi.org/10.1016/B978-0-12-385938-9.00057-2>
- Wilson G, Wilson TM, Deligne NI, Cole JW (2014) Volcanic hazard impacts to critical infrastructure: A review. *J Volcanol Geotherm Res* 286:148–182. <https://doi.org/10.1016/j.jvolgeores.2014.08.030>
- Wilson T, Stewart C, Cole J, Johnston D, Cronin S (2010) Vulnerability of farm water supply systems to volcanic ash fall. *Environ Earth Sci* 61:675–688. <https://doi.org/10.1007/s12665-009-0380-2>
- Zuccaro G, Cacace F, Spence RJS, Baxter PJ (2008) Impact of explosive eruption scenarios at Vesuvius. *J Volcanol Geotherm Res* 178:416–453. <https://doi.org/10.1016/j.jvolgeores.2008.01.005>